Crucial Role of Rho-Kinase in Pressure Overload–Induced Right Ventricular Hypertrophy and Dysfunction in Mice

Shohei Ikeda, Kimio Satoh, Nobuhiro Kikuchi, Satoshi Miyata, Kota Suzuki, Junichi Omura, Toru Shimizu, Kenta Kobayashi, Kazuto Kobayashi, Yoshihiro Fukumoto, Yasuhiko Sakata, Hiroaki Shimokawa

Objective—Right ventricular (RV) failure is the leading cause of death in various cardiopulmonary diseases, including pulmonary hypertension. It is generally considered that the RV is vulnerable to pressure overload as compared with the left ventricle (LV). However, as compared with LV failure, the molecular mechanisms of RV failure are poorly understood, and hence therapeutic targets of the disorder remain to be elucidated. Thus, we aimed to identify molecular therapeutic targets for RV failure in a mouse model of pressure overload.

Approach and Results—To induce pressure overload to respective ventricles, we performed pulmonary artery constriction or transverse aortic constriction in mice. We first performed microarray analysis and found that the molecules related to RhoA/Rho-kinase and integrin pathways were significantly upregulated in the RV with pulmonary artery constriction compared with the LV with transverse aortic constriction. Then, we examined the responses of both ventricles to chronic pressure overload in vivo. We demonstrated that compared with transverse aortic constriction, pulmonary artery constriction caused greater extents of mortality, Rho-kinase expression (especially ROCK2 isoform), and oxidative stress in pressure-overloaded RV, reflecting the weakness of the RV in response to pressure overload. Furthermore, mice with myocardial-specific overexpression of dominant-negative Rho-kinase showed resistance to pressure overload–induced hypertrophy and dysfunction associated with reduced oxidative stress. Finally, dominant-negative Rho-kinase mice showed a significantly improved long-term survival in both pulmonary artery constriction and transverse aortic constriction as compared with littermate controls.

Conclusion—These results indicate that the Rho-kinase pathway plays a crucial role in RV hypertrophy and dysfunction, suggesting that the pathway is a novel therapeutic target of RV failure in humans. **(*Arterioscler Thromb Vasc Biol*. 2014;34:1260-1271.)**

Key Words: heart failure, right-sided ■ hypertrophy, right ventricular ■ oxidative stress ■ rho-associated kinases

Pulmonary arterial hypertension is a fatal disease characterized by pulmonary vascular remodeling and resultant pressure overload to the right ventricle (RV) and RV failure. During the development of pulmonary arterial hypertension, the RV shows compensatory hypertrophy to maintain physiological wall stress, dilates with fibrotic changes, and ultimately results in functional failure.[1,2] However, as compared with left ventricular (LV) failure, the molecular mechanisms of RV failure are poorly understood, and hence therapeutic targets of the disorder remain to be elucidated.

The origin of the RV is developmentally different from that of the LV.[3] Therefore, many structural differences exist between the RV and the LV and it is generally considered that the RV is vulnerable to pressure overload but is resistant to volume overload and vice versa for the LV.[4,5] However, it remains to be examined how differently the RV responds to pressure overload as compared with the LV. To our knowledge, no studies have compared the differences in the responses to pressure overload between the 2 ventricles, with a special reference to underlying molecular mechanisms.

Pressure overload, such as systemic and pulmonary hypertension and stenotic valvular heart diseases, induces cardiac hypertrophy.[2,6,7] Although cardiac hypertrophy is basically a compensatory response to maintain wall stress, it eventually leads to cardiac dysfunction.[1,2,8,9] The responses of cardiac tissues to pressure overload are mediated by various intracellular signaling pathways, including oxidative stress–mediated signaling pathways.[10–13] We and others have previously demonstrated that the Rho-kinase pathway is substantially involved in LV pressure overload.[14,15] Although most of the previous studies focused on the responses of LV to pressure overload, the molecular mechanisms of RV failure remain poorly

Received on: January 21, 2014; final version accepted on: March 18, 2014.

From the Department of Cardiovascular Medicine, Tohoku University Graduate School of Medicine, Sendai, Japan (S.I., K.S., N.K., S.M., K.S., J.O., T.S., Y.F., Y.S., H.S.); and Department of Molecular Genetics, Institute of Biomedical Sciences, Fukushima Medical University School of Medicine, Fukushima, Japan (Ke. Kobayashi, Ka. Kobayashi).

This manuscript was sent to Qingbo Xu, Consulting Editor, for review by expert referees, editorial decision, and final disposition.

The online-only Data Supplement is available with this article at http://atvb.ahajournals.org/lookup/suppl/doi:10.1161/ATVBAHA.114.303320/-/DC1.

Correspondence to Hiroaki Shimokawa, MD, PhD, Department of Cardiovascular Medicine, Tohoku University Graduate School of Medicine, 1-1 Seiryocho, Aoba-ku, Sendai 980-8574, Japan. E-mail shimo@cardio.med.tohoku.ac.jp

Nonstandard Abbreviations and Acronyms	
DN-RhoK	dominant-negative Rho-kinase
ERK	extracellular signal-regulated kinase
LV	left ventricular
PAC	pulmonary artery constriction
RV	right ventricular
TAC	transverse aortic constriction

understood, and hence the therapeutic targets of RV failure remain to be elucidated.

In the present study, we thus aimed to elucidate the molecular mechanisms of pressure overload–induced RV failure by comparing the responses of both ventricles in mice. For this purpose, we used pulmonary artery constriction (PAC) and transverse aortic constriction (TAC) to induce pressure overload in the RV and the LV, respectively.

Materials and Methods

Materials and Methods are available in the online-only Supplement.

Results

Microarray Analysis

We first performed microarray analysis to examine the molecular signaling targets that could explain the difference in response to pressure overload between the RV (PAC) and the LV (TAC). By using the Ingenuity Pathway Analysis software, we found significant upregulation of integrin-β and integrin-β–related adhesion molecules (eg, α-actinin, talin, and vinculin) in the RV after PAC as compared with the LV after TAC (Table 1). The mechanotransduction through integrin may cause remodeling of actin cytoskeleton.[16,17] Thus, the significant upregulation of integrin-β–related adhesion molecules potentially reflects the characteristics of the RV that is vulnerable to tensile compared with the LV. We also found significant upregulation of the Rho/Rho-kinase–related genes only in the RV after PAC (Table 1). We also found that RhoA, a key molecule in the Rho/Rho-kinase pathway, was significantly upregulated in both PAC and TAC. Furthermore, ROCK1 and ROCK2 were differently regulated; ROCK2 was significantly increased only in the RV after PAC, whereas ROCK1 was unchanged in both ventricles (Table 1). To further evaluate the role of these pathways, we confirmed the top 15 gene expressions of Table 1 by real-time PCR (Figure II in the online-only Data Supplement). Consistent with the array data, the gene expressions in the RV after PAC showed significant increase as compared with the controls.

PAC and TAC Induces Oxidative Stress and Rho-Kinase Activation

To compare the responses of both ventricles to pressure overload, we performed PAC and TAC in wild-type mice. Importantly, mortality <24 hours was significantly higher in PAC compared with TAC, reflecting the vulnerability of the RV to acute pressure overload (Figure 1A). Oxidative stress is substantially involved in the development of cardiac hypertrophy and failure.[18–20] However, the time course and localization of oxidative stress induction in RV and LV after pressure overload remain to be examined. As evaluated by dihydroethidium staining at 24 hours after PAC and TAC in wild-type mice, we found rapid induction of oxidative stress in the loaded ventricles (Figure 1B; Figure IIIA in the online-only Data Supplement). PAC induced oxidative stress in the RV free wall, especially in the endocardium and epicardium, with no significant change in LV. In contrast, TAC induced oxidative stress in the LV wall, with no significant change in RV (Figure 1B, arrows).

We furthermore examined the changes in expressions of oxidative stress–related genes and Rho/Rho-kinase–related genes in the RV and LV at 24 hours after pressure overload by quantitative real-time PCR. Notably, oxidative stress genes (eg, p47phox and NOX2) were significantly upregulated in the RV after PAC and in the LV after TAC compared with the sham group (Figure 1C). Although there was no significant change in ROCK1 expression in loaded ventricles, RhoA and ROCK2 expressions were significantly upregulated in the loaded ventricles, which paralleled with the gene induction of p47phox and NOX2 (Figure 1C).

The roles of Rho-kinase (ROCK1 and ROCK2) in the LV and the RV after pressure overload remain to be elucidated. Thus, we next examined the time course and localization of ROCK1 and ROCK2 expression in the RV and the LV after PAC and TAC in wild-type mice by immunofluorescence staining (Figure 2B; Figure IIIB in the online-only Data Supplement). Interestingly, PAC rapidly and potently induced ROCK2 expression (but not ROCK1 expression) in the RV free wall, especially in the endocardium and free wall, at days 1 and 3, which was not evident in the LV (Figure 2B, arrows). In contrast, TAC induced ROCK1 expression at days 3 and 7 and ROCK2 expression at day 7 in the vascular wall and perivascular area (Figure 2A, arrows). In addition, we examined the protein levels of ROCK1 and ROCK2 by Western blotting (Figure IV in the online-only Data Supplement). Importantly, the protein levels of ROCK2 were upregulated at days 1 and 3 after PAC and at day 3 after TAC. Whereas, the protein levels of ROCK1 were gradually increased after PAC and TAC. Especially, the ROCK1 level at day 7 after TAC was significantly upregulated. We also found that the protein levels of ROCK1 (but not those of ROCK2) were significantly upregulated at 4 weeks after PAC and TAC. Furthermore, because the Rho-kinase staining patterns were similar to the localization of oxidative stress at day 1 after PAC (Figure 1A), we further examined the relationship between oxidative stress and Rho-kinase expressions by double-immunostaining. Interestingly, we noted the colocalizations of oxidative stress and ROCK2 (but not ROCK1) in the RV free wall at day 1 after PAC (Figure VA and VB in the online-only Data Supplement).

We further examined the relationship between Rho-kinase expressions and CD45-positive inflammatory cell migration by double-immunostaining (Figures VIA and VII in the online-only Data Supplement). Interestingly, PAC rapidly induced ROCK2 (but not ROCK1) expression exclusively in the RV wall, accompanied with CD45-positive inflammatory cell migration. In contrast, TAC slowly induced ROCK1 and ROCK2 in the perivascular wall, accompanied with

Table 1. List of Top 50 Genes Associated With the Integrin/Rho/Rho-Kinase Pathway at 24 h After Operation

Symbol	Gene ID	Description	PAC/Sham (RV, fold)	*P* Value	TAC/Sham (LV, fold)	*P* Value
Actn1	134156	Actinin, α1	14.346	<0.001	1.850	0.006
Itgb2	8404	Integrin, β2	11.525	<0.001	2.786	0.010
Fgd2	13710	FYVE, RhoGEF, and PH domain containing 2	3.440	<0.001	1.542	0.021
Itgb1	10578	Integrin, β1	2.962	<0.001	1.156	0.147
Actb	7393	Actin, β	2.921	<0.001	1.041	0.712
Ilk	1161724	Integrin-linked kinase	2.351	<0.001	1.302	0.002
Flna	10227	Filamin A, α	2.312	<0.001	0.979	0.836
Cdc42	9861	Cell division cycle 42	2.137	<0.001	1.151	0.021
Limk1	10717	LIM domain kinase 1	2.119	<0.001	1.668	0.005
Tln1	11602	Talin-1	2.026	<0.001	1.087	0.301
Vcl	9502	Vinculin	2.011	<0.001	1.114	0.323
Arhgef1	1130150	Rho guanine nucleotide exchange factor 1	1.830	0.021	1.384	0.030
Gata4	8092	GATA binding protein 4	1.774	0.008	1.512	0.005
Rock2	9072	Rho-associated, coiled-coil containing protein kinase 2	1.697	<0.001	1.056	0.573
Ppp1r12a	27892	Protein phosphatase 1, regulatory subunit 12A	1.647	0.019	0.828	0.223
Actr2	146243	Actin-related protein 2	1.552	<0.001	1.028	0.776
Vav3	20505	Vav 3 guanine nucleotide exchange factor 3	1.440	0.044	0.868	0.140
Rhoa	16802	Ras homolog family member A	1.407	<0.001	0.933	0.391
Rac1	9007	RAS-related C3 botulinum substrate 1	1.367	0.008	1.283	0.002
Parva	20606	Parvin, α	1.366	0.003	1.024	0.933
Parvb	133167	Parvin, β	1.339	0.003	1.114	0.280
Pkn2	178654	Protein kinase N2	1.309	0.006	0.934	0.111
Arhgef2	8487	Rho guanine nucleotide exchange factor 2	1.267	0.013	0.951	0.420
Pkn1	177262	Protein kinase N1	1.252	0.155	1.082	0.580
Fgd1	8001	FYVE, RhoGEF and PH domain containing 1	1.248	0.176	1.471	0.037
Ptk2	7982	Focal adhesion kinase	1.233	0.118	0.961	0.413
Pip5k1a	8847	Phosphatidylinositol-4-phosphate 5-kinase, type I, α	1.084	0.004	0.861	0.002
Rock1	9071	Rho-associated, coiled-coil containing protein kinase 1	0.918	0.313	1.095	0.546
Pik3ca	8839	Phosphatidylinositol-4,5-bisphosphate 3-kinase, catalytic subunit α	0.786	0.029	0.941	0.512
Arhgef10	172751	Rho guanine nucleotide exchange factor 10	0.783	0.006	1.299	0.023
Arhgef11	1003912	Rho guanine nucleotide exchange factor 11	0.782	0.032	1.050	0.637
Arhgef6	152801	Rho guanine nucleotide exchange factor 6	0.780	0.009	0.838	0.002
Prkca	11101	Protein kinase C, α	0.760	<0.001	0.801	0.117
Pten	80905	Phosphatase and tensin homolog	0.753	0.045	0.711	0.049
Pip5kl1	198191	Phosphatidylinositol-4-phosphate 5-kinase-like 1	0.738	0.013	0.933	0.705
Arhgef12	27144	Rho guanine nucleotide exchange factor 12	0.729	0.014	0.791	0.043
Tnnt1	11618	Troponin T type 1	0.726	0.037	0.642	0.063
Fgd5	172731	FYVE, RhoGEF and PH domain containing 5	0.663	0.003	1.153	0.333
Pld1	1164056	Phospholipase D1, phosphatidylcholine-specific	0.648	0.006	1.165	0.430
Itga1	1033228	Integrin, α1	0.645	0.027	0.914	0.456
Fgd4	139232	FYVE, RhoGEF and PH domain containing 4	0.642	0.019	0.625	0.024
Arhgef3	27871	Rho guanine nucleotide exchange factor 3	0.626	<0.001	0.976	0.771
Tnnt2	11619	Troponin T type 2	0.607	0.060	0.805	0.120
Mapk1	11949	Mitogen-activated protein kinase 1	0.598	0.002	0.688	0.015

(*Continued*)

Table 1. Continued

Symbol	Gene ID	Description	PAC/Sham (RV, fold)	*P* Value	TAC/Sham (LV, fold)	*P* Value
Rhpn2	27897	Rhophilin, Rho GTPase binding protein 2	0.588	<0.001	0.889	0.142
Arhgef19	172520	Rho guanine nucleotide exchange factor 19	0.574	<0.001	0.997	0.991
Plekhg5	1004156	Pleckstrin homology domain-containing family G member 5	0.555	<0.001	0.785	0.031
Farp2	145519	FERM, RhoGEF and pleckstrin domain protein 2	0.539	<0.001	0.875	0.301
Arhgef17	1081116	Rho guanine nucleotide exchange factor 17	0.437	0.002	0.924	0.576
Arhgef9	1033329	Rho guanine nucleotide exchange factor 9	0.272	<0.001	0.833	0.206

The number of samples is 4 in all groups. LV indicates left ventricle; PAC, pulmonary artery constriction; RhoGEF, Rho guanine nucleotide exchange factors; RV, right ventricle; and TAC, transverse aortic constriction.

CD45-positive inflammatory cell migration. Consistently, we noted significant increase in inflammatory gene expressions (interleukin-6, interleukin-1β, and tumor necrosis factor-α) in the loaded ventricles, especially in the RV wall, at day 1 after PAC (Figure VIB in the online-only Data Supplement), suggesting that the induction of ROCK2 and inflammation in response to pressure overload is greater in the RV compared with the LV. Consistently, we noted significant increase in tissue hypoxia in the loaded ventricles, especially in the RV, at day 3 after PAC (Figure 3A; Figure VIIIA in

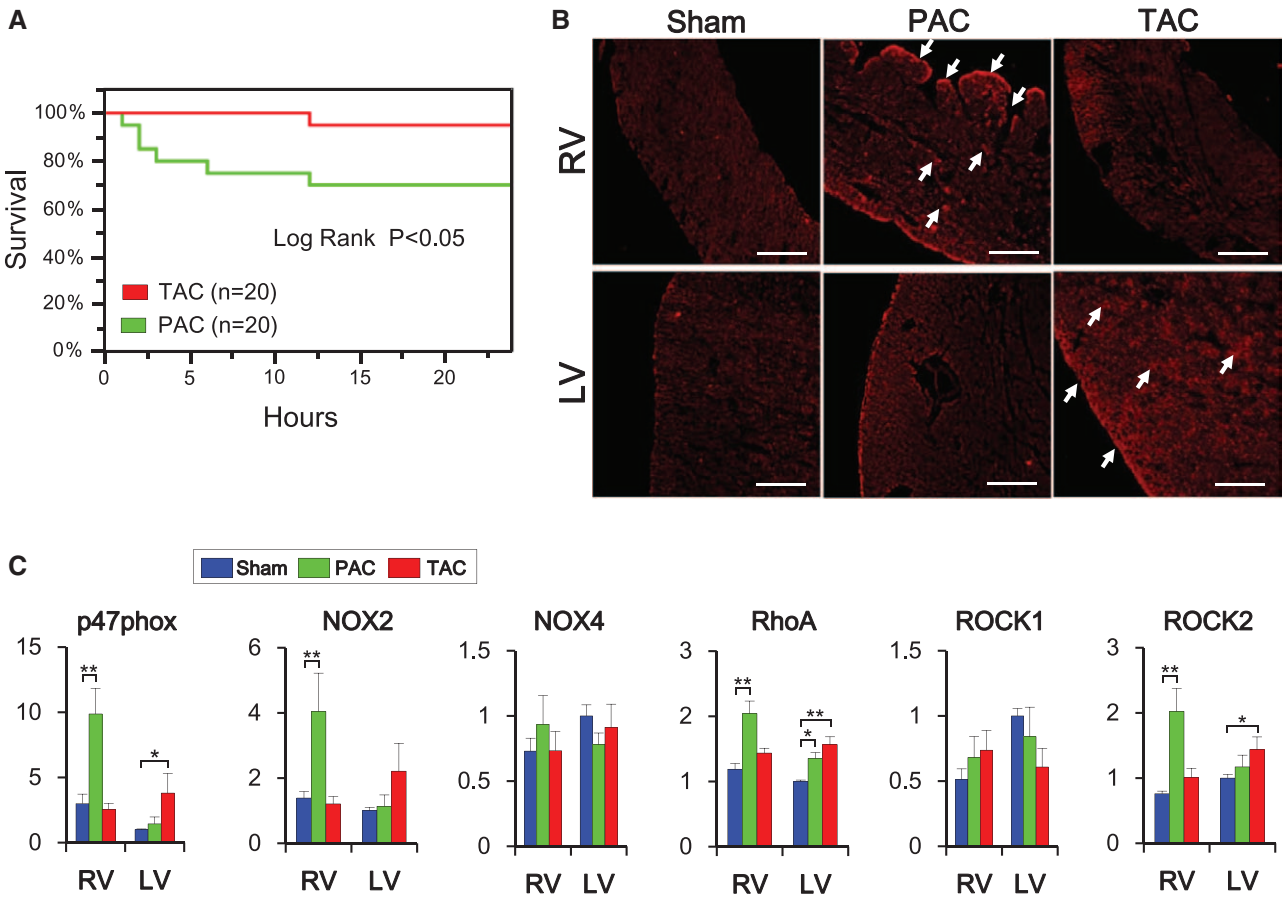

Figure 1. Pressure overload–induced oxidative stress in the ventricles. **A**, Survival curves <24 h showed higher mortality rates after pulmonary artery constriction (PAC) compared with transverse aortic constriction (TAC; n=20 each). **B**, Representative pictures of dihydroethidium staining of right ventricle (RV) and left ventricle (LV) 24 h after PAC or TAC. PAC induced strong oxidative stress in the RV, especially in the endocardium and epicardium (arrows), with no significant change in the LV. In contrast, TAC induced mild oxidative stress in the LV (arrows), with no significant change in the RV. Scale bars, 200 μm. **C**, Relative mRNA expressions of oxidative stress markers (p47phox, NOX2, and NOX4), Rho and Rho-kinases (ROCK1 and ROCK2) in RV and LV 24 h after PAC or TAC compared with control (n=10–12). There were significant upregulations in p47phox and NOX2 expressions in the RV after PAC and in the LV after TAC, especially higher after PAC. NOX4 expression was not significantly altered. There were similar upregulations in RhoA and ROCK2 expressions in pressure-loaded ventricles, whereas ROCK1 expression was not significantly altered. Results are adjusted by GAPDH. Results are expressed as mean±SEM. **P*<0.05; ***P*<0.01

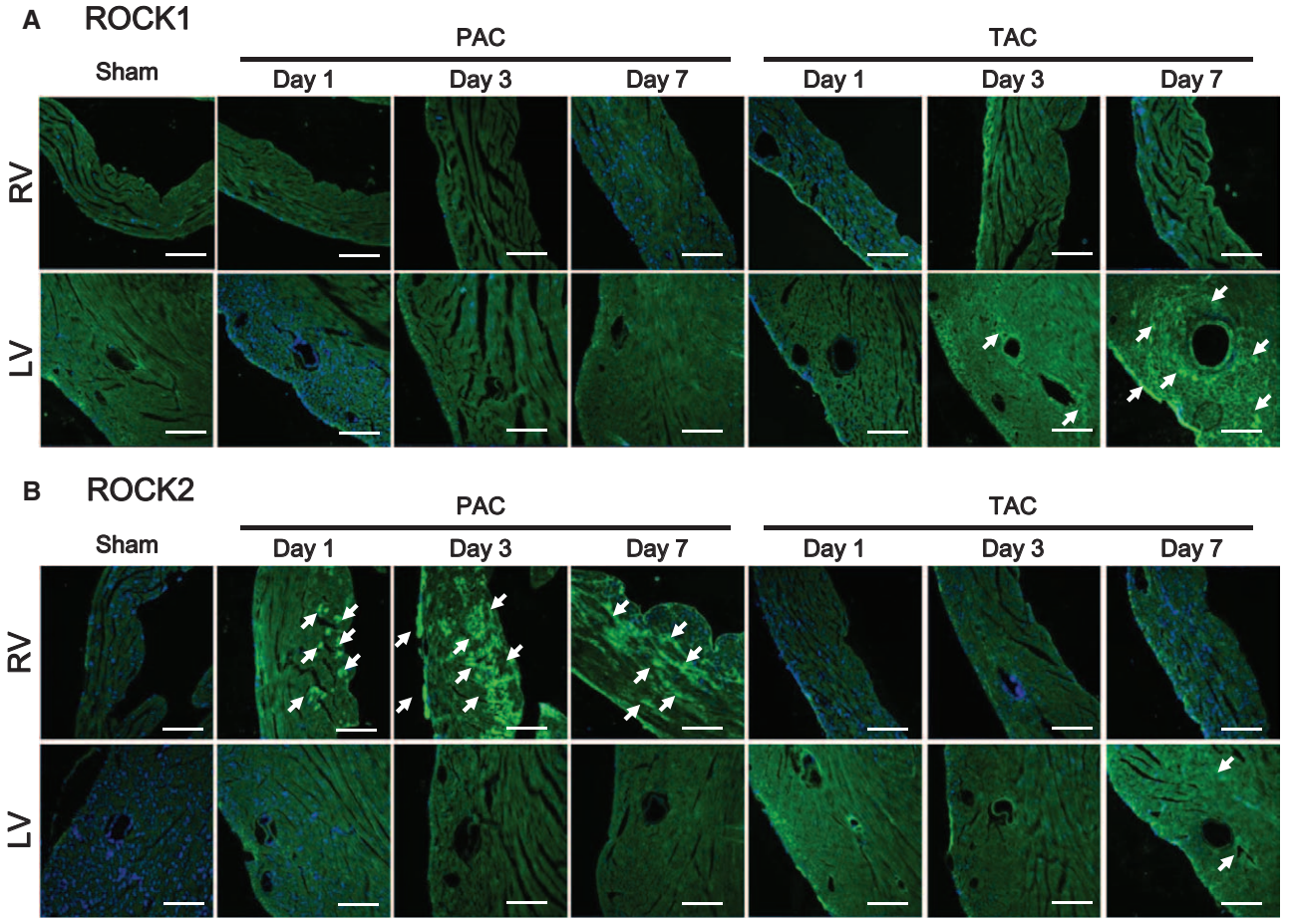

Figure 2. Pressure overload–induced upregulation of Rho-kinases in the ventricles. Representative photomicrographs of immunostaining showing time course and localization of ROCK1 and ROCK2 expression in the right ventricle (RV) and the left ventricle (LV) after pulmonary artery constriction (PAC) or transverse aortic constriction (TAC). **A**, There was no significant change in ROCK1 expression (ROCK1, green; DAPI, blue) at day 1 after PAC or TAC. However, TAC progressively induced ROCK1 expression especially in the vascular wall and perivascular area at day 7 (arrows). **B**, PAC quickly and potently induced ROCK2 expression in RV free wall especially in the endocardium and free wall (arrows), which was not observed in the LV (days 1 and 3). In contrast, TAC induced mild ROCK2 expression (ROCK2, green; DAPI, blue) in the LV, but not in the RV. TAC induced moderate ROCK 2 expression in the vascular wall (days 1 and 3). Scale bars, 200 μm.

the online-only Data Supplement). Both PAC and TAC progressively induced hypertrophic response (Figure 3B; Figure VIIIB in the online-only Data Supplement), and in parallel to it, TAC increased the capillary density in the LV (Figure 3C; Figure VIIIC in the online-only Data Supplement). In contrast, PAC did not increase capillary density in the RV, causing myocardial ischemia in the loaded RV (Figure 3A and 3C; Figure VIIIC in the online-only Data Supplement). These results suggest that the RV is more vulnerable to pressure overload and is more prone to myocardial ischemia as compared with the LV.

Crucial Role of Rho-Kinase for Cardiac Hypertrophy and Fibrosis in Pressure Overload

To further evaluate the role of myocardial Rho-kinase in response to pressure overload, we newly generated dominant-negative Rho-kinase (DN-RhoK) mice and examined the effects of PAC and TAC in those mice. In sham-operated mice, there was no difference in cardiac morphology between DN-RhoK mice and controls (Figure 4A and 4B). Although PAC caused RV hypertrophy and fibrosis in both genotypes (Figure 4A), the extent of the increase in RV cross-sectional area and interstitial fibrosis was significantly less in DN-RhoK mice than in controls (Figure 4B). Interestingly, PAC significantly reduced LV cross-sectional area in controls (Figure 4B), suggesting an unloaded influence of PAC on the LV. Similarly, although TAC caused progressive LV hypertrophy and fibrosis in both genotypes (Figure 4A), the extent of the increase in LV cross-sectional area and interstitial fibrosis was significantly less in DN-RhoK mice than in controls (Figure 4B). Importantly, we found that the changes in hypertrophy and fibrosis were significantly greater in PAC compared with TAC (Figure 4A and 4B). We further examined gene expressions of cardiac stress markers in both ventricles at 4 weeks after pressure overload (Figure 4C). The expressions of hypertrophic markers, such as atrial natriuretic factor and B-type natriuretic peptide, and fibrotic markers, such as collagen-I, III, and connective tissue growth factor, were significantly increased in loaded ventricles in both genotypes (Figure 4C). However, these increases in gene expressions in loaded ventricles were significantly less in DN-RhoK mice compared with controls (Figure 4C).

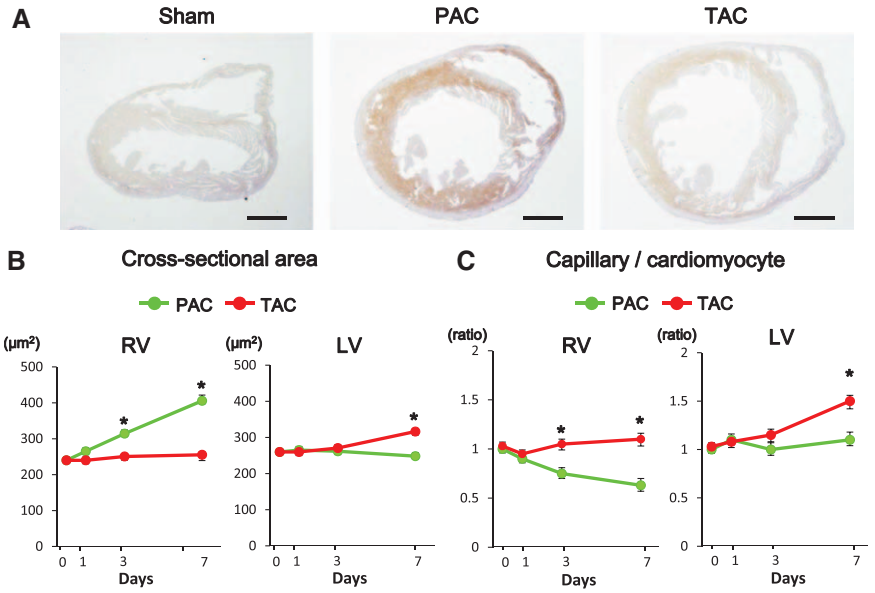

Figure 3. Pressure overload–induced cardiac hypertrophy and relative ischemia. **A**, Representative photomicrographs of a hypoxyprobe staining in the whole hearts at day 3 after pulmonary artery constriction (PAC), transverse aortic constriction (TAC), or sham, showing cardiac ischemic change induced by PAC and TAC (especially in the former). Scale bars, 1 mm. **B**, The time course of cross-sectional area of cardiomyocytes in the right ventricle (RV) and left ventricle (LV), showing that both PAC and TAC progressively induced hypertrophic response. **C**, The time course of capillary density in the RV and the LV, showing that PAC decreased the capillary density in the RV, whereas TAC increased it in the LV. Finally, these changes resulted in myocardial ischemia in pressure-overloaded ventricles. Capillary density was defined as the capillary to cardiomyocyte ratio. Results are expressed as mean±SEM. *P<0.05 vs day 0.

The measurement of organ weights showed that PAC significantly increased RV weight and reduced LV plus septum weight at 4 weeks after operation (Table II in the online-only Data Supplement). In contrast, TAC increased LV plus septum weight in controls, which was significantly less in DN-RhoK mice. We also found significant increase in liver weight (Table II in the online-only Data Supplement) and serum levels of liver enzymes (Table III in the online-only Data Supplement) after PAC compared with TAC, suggesting that PAC induced hepatic venous congestion. In contrast, TAC increased lung weight in both genotypes, suggesting lung congestion. However, these changes were significantly less in DN-RhoK mice compared with controls, suggesting a crucial role of Rho-kinase in response to preload as well as pressure overload.

Involvement of Rho-Kinase in Impaired Cardiac Function and Survival in Pressure Overload

We next performed echocardiographic examination in DN-RhoK mice and controls at 4 weeks after PAC and TAC (Figure 5A and 5B). In sham-operated mice, there was no difference in cardiac functions between DN-RhoK mice and controls (Figure 5A and 5B). Notably, PAC caused RV dilatation and dysfunction in both genotypes with paradoxical motion of interventricular septum (Figure 5A). However, the increase in RV internal diameter in diastole and the decrease in RV fractional shortening were significantly less in DN-RhoK mice compared with controls (Figure 5B). In contrast, TAC caused LV dilatation and dysfunction in both genotypes. However, the increase in LV end-diastolic diameter and the decrease in LV fractional shortening were significantly less in DN-RhoK mice compared with controls (Figure 5B). TAC did not induce significant changes in RV internal diameter in diastole or RV fractional shortening (Figure 5B). The decrease in cardiac output was noted in both models, which was also significantly ameliorated in DN-RhoK mice compared with controls (Figure 5B).

To further examine cardiac functions after PAC and TAC, we performed catheter examinations at 4 weeks after operation (Table 2). DN-RhoK mice and controls showed equal increase in RV systolic blood pressure after PAC (Table 2). Furthermore, PAC significantly increased end-diastolic pressure in both ventricles of both genotypes; however, the increases were significantly less in DN-RhoK mice compared with controls. In contrast, DN-RhoK mice and controls showed equal increase in LV systolic blood pressure after TAC (Table 2). Although TAC significantly increased RV systolic blood pressure in both genotypes, the increase was significantly less in DN-RhoK mice compared with controls. Furthermore, although TAC significantly increased end-diastolic pressure in both ventricles of both genotypes, these increases were significantly less in DN-RhoK mice compared with controls. Inconsistent with the hemodynamic results, we found significantly improved survival rates in DN-RhoK mice compared with controls in both PAC and TAC models (Figure 5C).

Rho-Kinase Activates Extracellular Signal-Regulated Kinase 1/2 and GATA4 in Loaded Ventricles

Pressure overload rapidly and potently induced oxidative stress and Rho-kinase upregulations in loaded ventricles (Figures 1 and 2). To further examine the molecular responses to pressure overload, we examined myocardial Rho-kinase activity in loaded ventricles, as evaluated by the ratio of phosphorylated/total form of myosin-binding subunit (Figure 6A; Figure IX in the online-only Data Supplement). In sham-operated mice, myocardial Rho-kinase activity of both ventricles was significantly less (~30%) in DN-RhoK mice compared with controls. PAC and TAC significantly activated Rho-kinase in loaded ventricles at 4 weeks after operation, and this activation was significantly less in DN-RhoK mice compared with controls in both PAC and TAC models. In contrast, interestingly, in the contralateral ventricles to pressure overload (LV after PAC and RV after TAC), we found no Rho-kinase activation. Extracellular signal-regulated kinase (ERK) 1/2 is activated in the hypertrophic responses to pressure overload.[21,22] Because microarray analyses showed a significant increase in ERK and GATA4 expressions in response to pressure overload

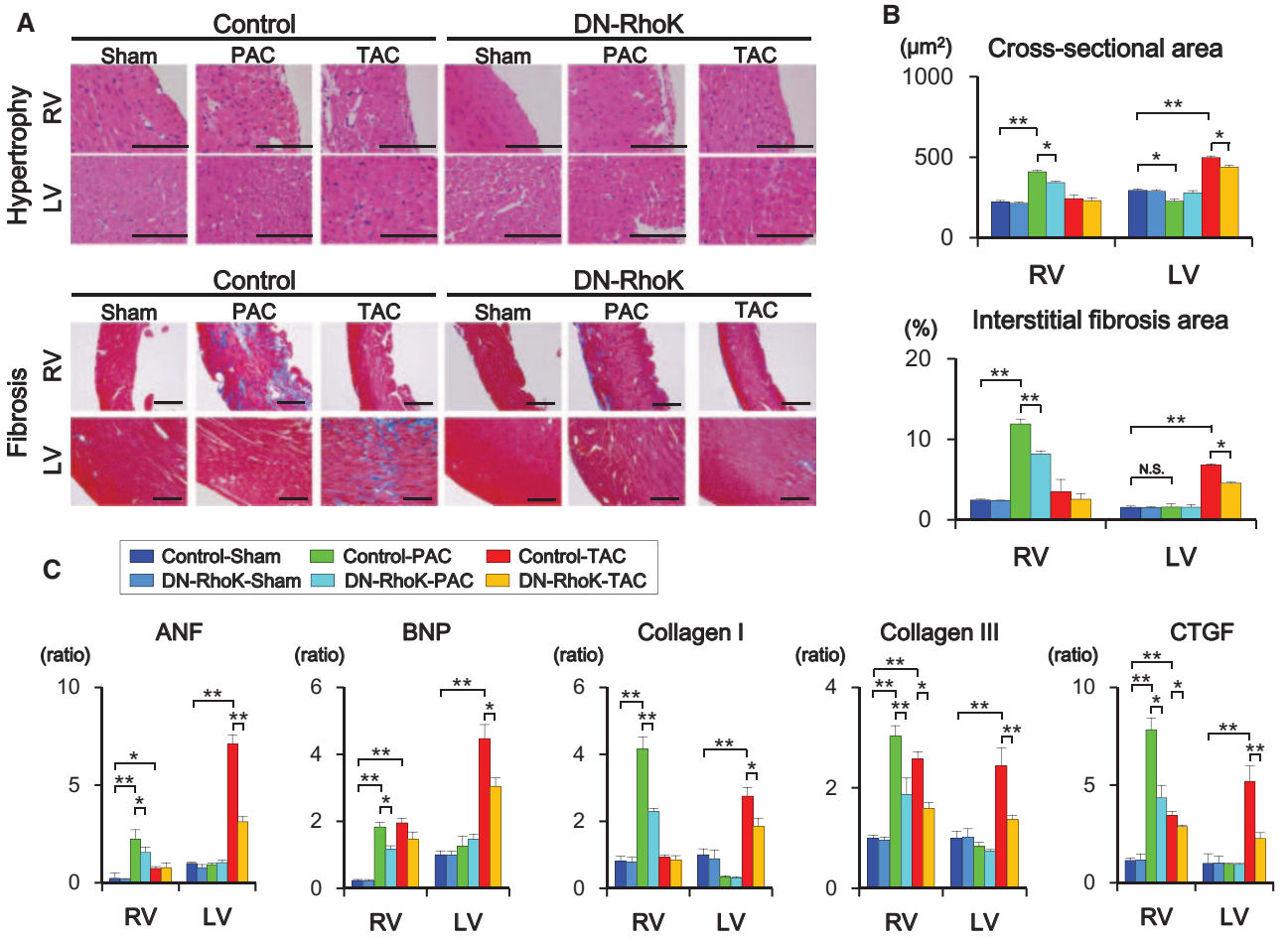

Figure 4. Crucial role of Rho-kinase for cardiac hypertrophy and fibrosis in the ventricles. **A**, Representative photomicrographs of HE staining (**top**) and Masson trichrome staining (MT staining; **bottom**) of the hearts in dominant-negative Rho-kinase (DN-RhoK) mice and controls 4 wk after pulmonary artery constriction (PAC) or transverse aortic constriction (TAC). Photomicrographs of HE staining show cardiac hypertrophy. Scale bars, 100 μm. Photomicrographs of MT staining show interstitial fibrosis. Scale bars, 200 μm. **B**, Quantitative analysis of cross-sectional area and interstitial fibrosis area of the right ventricle (RV) and the left ventricle (LV) in DN-RhoK mice and controls (n=6–10) 4 wk after operation. PAC and TAC induced significant hypertrophy and interstitial fibrosis in both genotypes; however, the extents of the increases were significantly less in DN-RhoK mice than in controls. Additionally, PAC significantly reduced the cross-sectional area of LV in controls. **C**, Relative mRNA expressions of hypertrophic markers, atrial natriuretic factor (ANF), and B-type natriuretic peptide (BNP), and fibrotic markers, collagen I and III, and connective tissue growth factor (CTGF) in the RV and the LV in DN-RhoK mice and controls (n=4–6) 4 wk after operation. The respective expressions of hypertrophic and fibrotic markers were significantly increased in pressure-overloaded ventricles in both genotypes. However, the extents of the increases were significantly less in DN-RhoK mice than in controls. Results are adjusted by GAPDH. Results are expressed as mean±SEM. *P<0.05; **P<0.01.

(Table 1), we examined the activity and nuclear translocation of p-ERK1/2 by immunostaining and Western blotting (Figure 6B and 6C). Interestingly, PAC and TAC increased the number of p-ERK1/2–positive nuclei in loaded ventricles (Figure 6B). Moreover, PAC and TAC activated ERK1/2 as assessed by the increase in p-ERK1/2 in the nuclear fraction in both genotypes (Figure 6C). However, this activation was significantly less in DN-RhoK mice compared with controls in both genotypes (Figure 6C).

We further examined the activity and nuclear translocation of GATA4, the downstream mediator of ERK1/2, in loaded ventricles. Both PAC and TAC activated GATA4 as assessed by the ratio (p/t GATA4) in loaded ventricles in both genotypes (Figure 6C). However, this activation and nuclear translocation were significantly less in DN-RhoK mice compared with controls in both models (Figure 6C). Taken together, these results indicate that pressure overload by PAC and TAC activate and nuclear-translocate ERK 1/2 and GATA4 in loaded ventricles, in which Rho-kinase is substantially involved.

Rho-Kinase Causes Oxidative Stress in Loaded Ventricles

We further examined oxidative stress induction in DN-RhoK mice and controls at 4 weeks after PAC and TAC. Dihydroethidium staining showed that PAC and TAC significantly induced oxidative stress in RV and LV, respectively, compared with sham-operated mice (Figure XA and XB in the online-only Data Supplement). However, the induction of oxidative stress was significantly less in DN-RhoK mice compared with controls in both PAC and TAC models (Figure XA and XB in the online-only Data Supplement). Importantly, the relative fluorescence of dihydroethidium staining showed that PAC induced greater extent of oxidative stress compared with TAC in controls (Figure XA and XB in the online-only

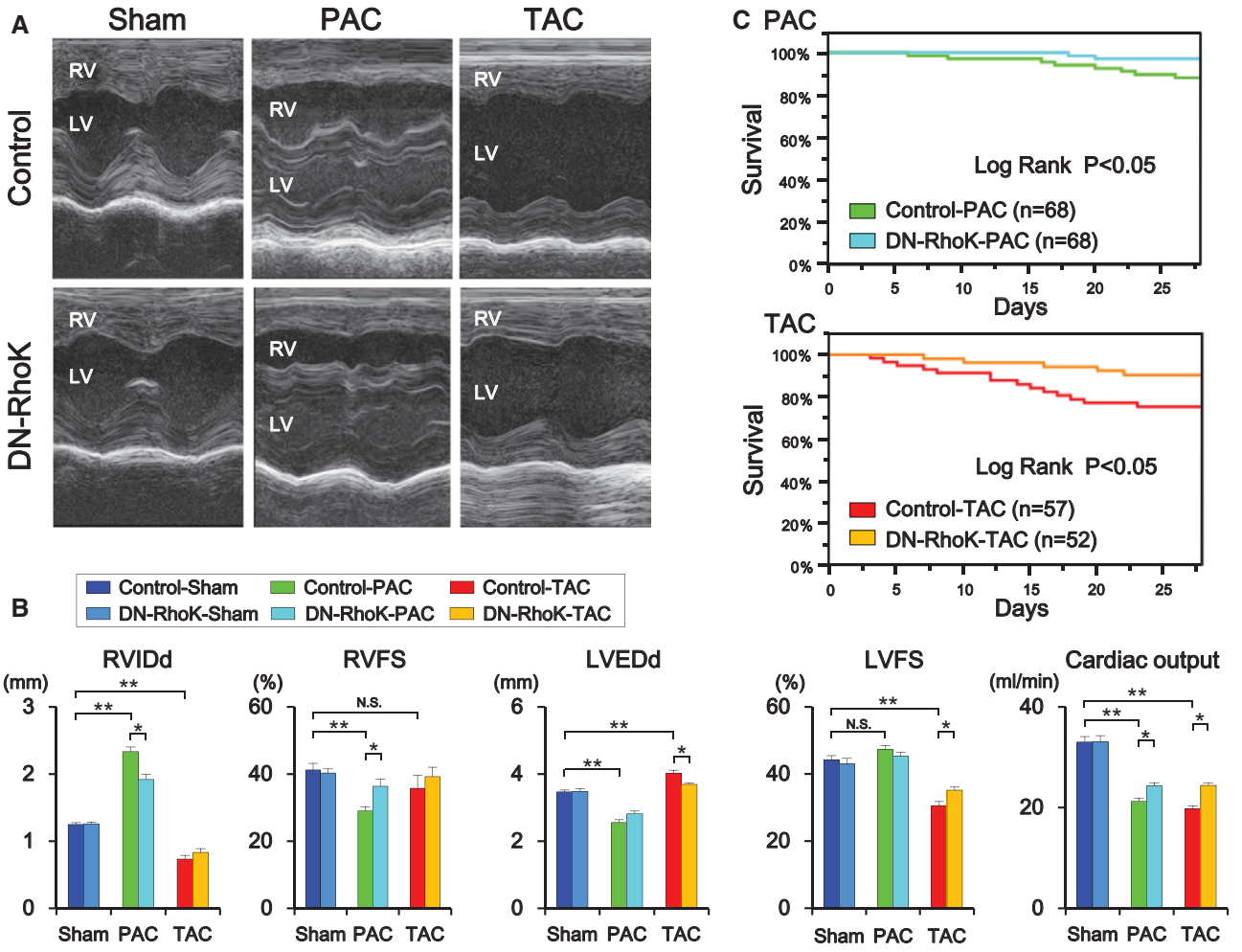

Figure 5. Involvement of Rho-kinase in pressure overload–induced cardiac dysfunction and reduced survival. **A**, Representative transthoracic M-mode echocardiographic tracings of the heart in dominant-negative Rho-kinase (DN-RhoK) mice and controls 4 wk after operation. Pulmonary artery constriction (PAC) caused right ventricle (RV) dilatation and dysfunction in both genotypes with paradoxical motion of the interventricular septum. In contrast, transverse aortic constriction (TAC) caused left ventricle (LV) dilatation and dysfunction in both genotypes. **B**, Quantitative analysis of the parameters of cardiac functions in DN-RhoK mice and controls (n=6≈10) at 4 wk after operation. PAC significantly increased RV internal diameter in diastole (RVIDd) and reduced RV fractional shortening (RVFS) and cardiac output; however, the levels of the respective changes were significantly less in DN-RhoK mice than in controls. In contrast, TAC significantly increased LV end-diastolic diameter (LVEDd) and reduced LV fractional shortening (LVFS) and cardiac output; however, the extents of the changes were significantly less in DN-RhoK mice than in controls. **C**, Long-term survival curves showed mortality rates ameliorated significantly in DN-RhoK mice compared with controls after PAC or TAC. The analysis was started after 24 h of respective operations. Results are expressed as mean±SEM. *P<0.05; **P<0.01.

Data Supplement). Oxidative stress induces autophagy in the pathogenesis of heart failure.[23] Thus, we finally examined autophagy by Western blotting for the autophagy markers LC3A and p62/SQSTM-1 (Figure XC and XD in the online-only Data Supplement). Importantly, both PAC and TAC significantly increased the levels of LC3A and p62/SQSTM-1 in loaded ventricles (Figure XC and XD in the online-only Data Supplement), and this increase was significantly less in DN-RhoK mice, suggesting that Rho-kinase plays a crucial role in the induction of cardiac oxidative stress and autophagy.

Discussion

The major findings of the present study are as follows: (1) The extent of upregulation of the molecules downstream of integrin-β and RhoA, both of which augment oxidative stress in pressure-overloaded ventricles, was greater in PAC compared with TAC (Figures XI and XII in the online-only Data Supplement). (2) ROCK2 was rapidly upregulated in the RV after PAC, colocalized with reactive oxygen species induction, whereas no significant change in ROCK1 expression was noted in pressure-overloaded ventricles. (3) Cardiac Rho-kinase plays a crucial role for the activation of ERK1/2–GATA4 signaling in response to pressure overload. (4) Rho-kinase, especially ROCK2, is substantially involved in the molecular mechanisms of RV dysfunction and impaired survival in response to pressure overload. To the best of our knowledge, this is the first study that demonstrates the possible therapeutic importance of the Rho-kinase pathway in RV failure.

Specific Responses of the RV to Pressure Overload

Although the structural difference between the 2 ventricles is obvious, the fundamental functional difference between RV

Table 2. Hemodynamic Data at 4 wk After Operation

	Sham		PAC		TAC	
Parameters	Control (n=6)	DN-RhoK (n=6)	Control (n=6)	DN-RhoK (n=6)	Control (n=6)	DN-RhoK (n=6)
HR, beats/min	499±22	481±37	502±33	508±19	490±12	507±21
RV systolic pressure, mm Hg	23.0±1.3	23.0±2.0	73.4±3.0**	72.8±3.3††	36.7±1.8**	32.0±1.4††,§
RV end diastolic pressure, mm Hg	1.86±0.4	1.92±0.3	4.10±0.8*	2.40±0.6‡	3.63±0.7*	2.22±0.5
LV systolic pressure, mm Hg	100.5±1.3	100.8±2.8	103.1±1.3	105.2±2.3	183.5±4.3**	185.5±3.5††
LV end diastolic pressure, mm Hg	2.1±0.6	2.5±0.6	12.2±0.5**	6.5±0.5††,‡‡	11.3±2.1**	7.2±1.1††,§

Results are expressed as mean±SEM. Comparisons were made using 1-way ANOVA. DN-RhoK indicates dominant-negative Rho-kinase; HR, heart rate; LV, left ventricle; PAC, pulmonary artery constriction; RV, right ventricle; and TAC, transverse aortic constriction.

*P<0.05, **P<0.01 vs sham-operated controls; †P<0.05, ††P<0.01 vs sham-operated DN-RhoK mice; ‡P<0.05, ‡‡P<0.01 vs controls with PAC; §P<0.05, §§P<0.01 vs controls with TAC.

failure and LV failure remains unclear.[4,5] Thus, we still have limited knowledge and strategy for the treatment of RV failure. In the present study, we addressed this fundamental issue by comparing the responses of both ventricles to pressure overload. Interestingly, there were significant differences in the induction pattern and localization of oxidative stress at 24 hours after pressure overload; PAC rapidly induced oxidative stress in the RV without significant change in the LV, whereas TAC slowly induced oxidative stress in the LV without significant change in the RV. Furthermore, ROCK2 was promptly

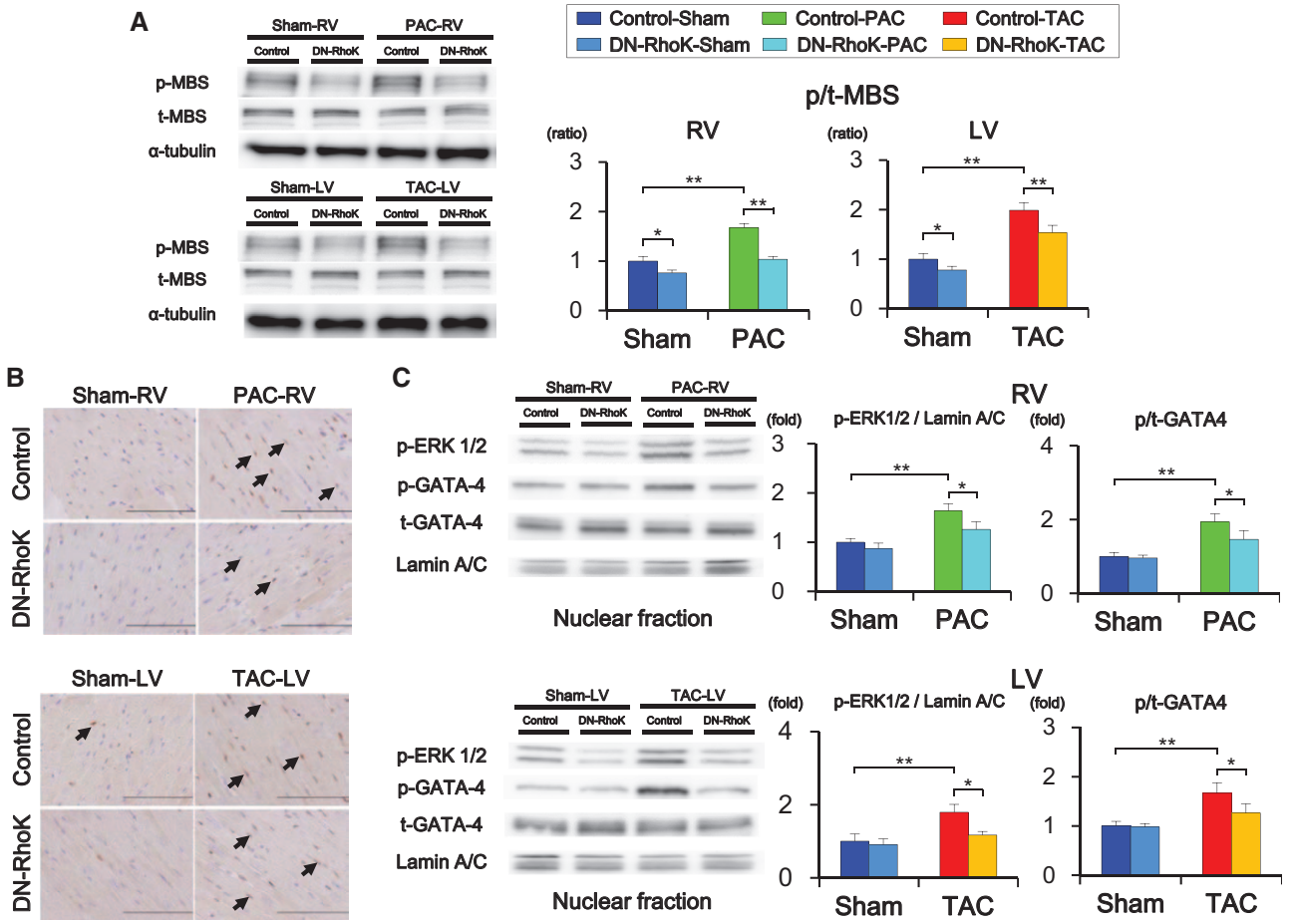

Figure 6. Rho-kinase activates myocardial extracellular signal-regulated kinase (ERK) 1/2 and GATA4 in response to pressure overload. **A**, Representative Western blotting photographs of phospho-MBS (p-MBS) and total MBS (t-MBS) and quantitative analysis of Rho-kinase activity in loaded ventricles 4 wk after operation (n=8 each). LV indicates left ventricle; and RV, right ventricle. Pulmonary artery constriction (PAC) and transverse aortic constriction (TAC) significantly activated Rho-kinase in pressure-loaded ventricles, and the respective activations were significantly less in dominant-negative Rho-kinase (DN-RhoK) mice compared with controls. **B**, Representative photomicrographs of immunostaining for phosphorylated ERK1/2 (p-ERK1/2) in loaded ventricles 4 wk after operation. PAC and TAC increased the number of p-ERK1/2-positive nuclei in pressure-loaded ventricles. Scale bars, 100 μm. **C**, Representative Western blotting of p-ERK1/2 and phospho-GATA4 (p-GATA4) and total GATA4 (t-GATA4) in nuclear fraction of loaded ventricles 4 wk after operation (n=5 each). PAC and TAC significantly activated ERK1/2 and GATA4 in the nuclei of loaded ventricles, and the respective activations were also significantly less in DN-RhoK compared with controls in both models. Results are expressed as mean±SEM. *P<0.05; **P<0.01.

upregulated in the RV after PAC, colocalized with reactive oxygen species induction. Interestingly, ROCK2-positive cardiomyocytes accompanied CD45-positive inflammatory cells, which would further augment oxidative stress and deteriorate the function of loaded ventricles (Figures XI and XII in the online-only Data Supplement). Thus, it is conceivable that the increased ROCK2 expression in the RV after PAC contributes, at least in part, to the vulnerability of the RV to pressure overload and the characteristic difference between the 2 ventricles. At present, we still have limited knowledge about the roles of ROCK1 and ROCK2 in the pathogenesis of RV and LV failure. However, recent reports revealed different roles of ROCK1 and ROCK2 in TAC-induced LV hypertrophy; ROCK1 plays an important role in fibrosis, whereas ROCK2 promotes hypertrophy.[24,25] Thus, the prompt and potent upregulation of ROCK2 in the pressure-overloaded RV may reflect the crucial role of cardiac ROCK2 for hypertrophic responses. Several studies have reported that the RV expresses α-myosin heavy chain (V1) isoform to a greater extent compared with the LV, associated with a higher ATPase activity.[26,27] This may link the pathogenetic role of ROCK2 in pressure-overloaded RV.

Regarding the upstream molecular mechanisms that augment ROCK2 expression in pressure-overloaded RV, the present microarray analysis revealed significant increases in integrin-β and its downstream mechanotransduction-related genes (eg, talin, vinculin, focal adhesion kinase, paxillin, and α-actinin) in the RV after PAC, but not in the LV after TAC. Mechanical stretch stimulates integrins, which activates RhoA/Rho-kinase signaling through Rho guanine nucleotide exchange factors.[28] Mechanotransduction through integrins leads to the activation of RhoA/Rho-kinase pathway, which induces hypertrophic gene activation.[16,17] In contrast, mechanosensing by actin filaments causes actin cytoskeleton remodeling through small GTPases of the Rho/Rac/Cdc42 family. However, the detailed mechanisms are not fully elucidated as to the mechanoresponses and the link between the integrin, Rho guanine nucleotide exchange factors, and the downstream target, RhoA/Rho-kinase signaling. In the downstream mechanotransduction through integrin-β by pressure overload, the adhesion of α-actinin, talin, and vinculin to actin filaments may potentially contribute to the activation of FGD2 (Rho guanine nucleotide exchange factor) preferentially in the RV after PAC.[16] The present microarray analysis suggests that there is a special signaling cascade in the RV that connects the FGD2 and RhoA/ROCK2 signaling to the downstream of integrin-β, which may be the difference between the RV and the LV in response to mechanical stretch. Further studies on the roles of FGD2 and ROCK2 in RV pressure overload are needed to better understand the pathogenesis of RV failure.

Although it is widely known that cardiomyocytes can sense mechanical forces, it remains largely unknown how the forces are transmitted through the cytoskeleton. Moreover, the molecular differences between RV and LV cardiomyocytes remain to be elucidated. The present study demonstrates how forces applied to the cardiomyocytes are molecularly transduced and shared by cytoskeleton and crosslinker proteins (Figures XI and XII in the online-only Data Supplement). Taken together, these results suggest that ROCK2 plays a central role in the development of pressure overload–induced RV failure.

Pressure Overload Activates ROCK2 in Loaded Ventricles

We and others have previously demonstrated that the Rho-kinase pathway is substantially involved in LV hypertrophy and failure in animals, in which oxidative stress is substantially involved.[14,15] In the present study, we showed that the induction pattern and localization of oxidative stress was similar to those of ROCK2 in the RV after PAC. Thus, we evaluated the therapeutic effects of inhibition of cardiac Rho-kinase in PAC-induced RV hypertrophy and dysfunction in comparison with TAC-induced LV hypertrophy and dysfunction. Because many ROCK substrates are involved in cell death processes,[29] systemic deletion of Rho-kinase is embryonic-lethal.[30] Thus, we newly generated and used mice with myocardial-specific overexpression of DN-RhoK in the present study. In the present study, pressure overload induced oxidative stress and caused cardiac hypertrophy, fibrosis, and failure in both ventricles. Importantly, the DN-RhoK mice showed significantly fewer changes in pressure-loaded ventricles and significantly improved survival in both PAC and TAC models.

It is widely accepted that ERK1/2 plays a crucial role in myocardial hypertrophic responses to pressure overload.[21,22] ERK1/2 signaling is associated with phosphorylation and activation of the cardiac prohypertrophic transcription factor GATA4.[31] Moreover, GATA4 regulates various gene expressions related to hypertrophy and heart failure.[32–34] Importantly, microarray analysis demonstrated that the expressions of both ERK and GATA4 were significantly upregulated in pressure-overloaded RV of wild-type mice. The present in vivo findings are in agreement with the previous in vitro studies.[35–37] It was previously reported that Rho-kinase contributes to the activation of ERK1/2 and GATA4 in myocardial hypertrophic response in vitro[35] and that Rho-kinase plays an important role in the nucleus translocation of p-ERK and GATA4 activation in vascular smooth muscle cells.[36,37] Taken together, the present study provides the first evidence that the ERK1/2–GATA4 signaling pathway is downregulated in DN-RhoK mice compared with controls, resulting in attenuated myocardial hypertrophy and dysfunction in both PAC and TAC models (Figures XI and XII in the online-only Data Supplement).

In the process of pressure overload and cardiac failure, oxidative stress promotes induction of mitochondrial damage and autophagy.[20] Autophagy is required for adaptive response to hemodynamic stress and is increased in failing hearts,[38] in which GATA4 activation is critically involved.[39] In the present study, autophagy was significantly increased in pressure-overloaded ventricles by PAC and TAC in control mice, which was again significantly attenuated in DN-RhoK mice. Thus, Rho-kinase enhances autophagy in pressure-overloaded ventricles during compensatory hypertrophic response and dysfunction in both ventricles. In the present study, the inhibition of ROCK2 similarly ameliorated TAC- and PAC-induced cardiac hypertrophy and dysfunction, suggesting the importance of ROCK2 in both ventricles. However, to the best of our knowledge, the present study is the first that demonstrated the important role of Rho-kinase in the RV, suggesting the potential therapeutic importance of Rho-kinase in RV failure. A Rho-kinase inhibitor, fasudil, has been demonstrated

to exert therapeutic effects in several cardiovascular diseases in animals and in humans.[40,41] These results implicate the potential usefulness of Rho-kinase inhibitors for the treatment of patients with pressure overload–related disorders, such as hypertenstive heart disease and valvular heart disease. In addition, the development of isoform-specific ROCK inhibitors, especially ROCK2 inhibitors, may also be promising for the treatment of cardiac hypertrophy and failure.[15,24]

Characteristics of RV Failure in Comparison With LV Failure

To our knowledge, there is a study demonstrating the different gene expressions after PAC and TAC in mice.[7] In the present study, we performed precise analyses, which further provided detailed characterizations of the difference between PAC and TAC. In the present study, the mortality of wild-type mice was better in TAC than in PAC in the acute phase, whereas the opposite was true in the chronic phase. In the present study, angiogenic response to pressure overload was less in the RV as compared with LV. Thus, it is possible that the extent of myocardial ischemia was greater in the RV than in the LV in the acute phase, as delineated with hypoxyprobe staining. Furthermore, the difference in the mortality could be explained by the present findings in PAC-induced RV failure. We found significant increase in liver weight after PAC, but not after TAC, a consistent finding with the previous report on hepatic venous congestion in PAC-induced RV failure.[7] Importantly, the increase in liver weight was significantly attenuated in DN-RhoK mice. In addition, PAC increased the serum levels of liver enzymes, as in the case with patients with severe RV failure.[42] Again, this was not the case for TAC. Interestingly, PAC significantly reduced LV weight, a consistent finding with the recent report that RV failure caused by pulmonary hypertension is associated with reduced LV free wall mass, probably because of negative ventricular–ventricular interaction and the long-term decrease in cardiac output.[43] Further studies are needed to elucidate the mechanisms involved in the alterations of the LV in response to RV pressure overload. Whereas, we found a significant increase in lung weight only in TAC, representative characteristics of lung remodeling and postcapillary pulmonary hypertension in LV failure.[8] One of the important characteristics of RV failure is the negative ventricular–ventricular interaction through the septum and epicardium with a resultant impairment of LV diastolic function.[44] Consistent with this report, we found an increase in LV diastolic pressure in the PAC model, suggesting LV diastolic dysfunction after PAC. Indeed, the RV is different from the LV structurally, geometrically, and mechanically.[2] In the present study, there were significant differences between PAC and TAC in terms of LV remodeling, capillary density, myocardial fibrosis, systolic blood pressure, lung and liver weights, and Rho-kinase activity, all of which may have affected the different mortality between the 2 models.

Study Limitations

Several limitations should be mentioned for the present study. First, pressure overload models with PAC or TAC may not fully represent the clinical features of RV and LV failure in humans. Thus, the present findings remain to be confirmed in other animal models of RV failure and finally in patients with the disorder. Second, although we ligated the aorta and pulmonary artery with the same needle (27G) for the same period (≈30 days), the extent of constriction of the arteries could have been incomparable because of the differences in their diameter, wall thickness, and physiology. Thus, we cannot eliminate the possibility that the difference between LV and RV responses could have been a technical issue. Third, because both ROCK1 and ROCK2 were inhibited in the present study by the overexpression of DN-RhoK, it remains to be determined which isoform is mainly responsible for the present findings, although the present results strongly suggest more important roles of ROCK2 as compared with ROCK1. These points also need to be examined in future studies using mice lacking respective isoform of Rho-kinase.

Conclusions

In the present study, we were able to demonstrate that the Rho-kinase pathway (especially ROCK2-mediated one) plays a crucial role in RV hypertrophy and dysfunction, suggesting that the pathway is a novel therapeutic target of RV failure in humans.

Acknowledgments

We are grateful to Dr T. Urashima at the Jikei University School of Medicine for technical advice on our work, and to Akemi Saito, Yumi Watanabe, Teru Hiroi, and Ai Nishihara in our laboratory for excellent technical assistance.

Sources of Funding

This work was supported in part by the grant-in-aid for Tohoku University Global COE for Conquest of Signal Transduction Diseases with Network Medicine and those for Scientific Research (21790698, 23659408, and 24390193), all of which are from the Japanese Ministry of Education, Culture, Sports, Science, and Technology (Tokyo, Japan), and the grants-in-aid for Scientific Research from the Japanese Ministry of Health, Labour, and Welfare (Tokyo, Japan; 10102895).

Disclosures

None.

References

1. Sandoval J, Bauerle O, Palomar A, Gómez A, Martínez-Guerra ML, Beltrán M, Guerrero ML. Survival in primary pulmonary hypertension. Validation of a prognostic equation. *Circulation*. 1994;89:1733–1744.
2. Bogaard HJ, Abe K, Vonk Noordegraaf A, Voelkel NF. The right ventricle under pressure: cellular and molecular mechanisms of right-heart failure in pulmonary hypertension. *Chest*. 2009;135:794–804.
3. Verzi MP, McCulley DJ, De Val S, Dodou E, Black BL. The right ventricle, outflow tract, and ventricular septum comprise a restricted expression domain within the secondary/anterior heart field. *Dev Biol*. 2005;287:134–145.
4. Walker LA, Buttrick PM. The right ventricle: biologic insights and response to disease. *Curr Cardiol Rev*. 2009;5:22–28.
5. Greyson CR. Pathophysiology of right ventricular failure. *Crit Care Med*. 2008;36(1 suppl):S57–S65.
6. Rockman HA, Ross RS, Harris AN, Knowlton KU, Steinhelper ME, Field LJ, Ross J Jr, Chien KR. Segregation of atrial-specific and inducible expression of an atrial natriuretic factor transgene in an *in vivo* murine model of cardiac hypertrophy. *Proc Natl Acad Sci U S A*. 1991;88:8277–8281.
7. Urashima T, Zhao M, Wagner R, Fajardo G, Farahani S, Quertermous T, Bernstein D. Molecular and physiological characterization of RV remodeling in a murine model of pulmonary stenosis. *Am J Physiol Heart Circ Physiol*. 2008;295:H1351–H1368.

8. Chen Y, Guo H, Xu D, Xu X, Wang H, Hu X, Lu Z, Kwak D, Xu Y, Gunther R, Huo Y, Weir EK. Left ventricular failure produces profound lung remodeling and pulmonary hypertension in mice: heart failure causes severe lung disease. *Hypertension*. 2012;59:1170–1178.
9. Hein S, Arnon E, Kostin S, Schönburg M, Elsässer A, Polyakova V, Bauer EP, Klövekorn WP, Schaper J. Progression from compensated hypertrophy to failure in the pressure-overloaded human heart: structural deterioration and compensatory mechanisms. *Circulation*. 2003;107:984–991.
10. Heineke J, Molkentin JD. Regulation of cardiac hypertrophy by intracellular signalling pathways. *Nat Rev Mol Cell Biol*. 2006;7:589–600.
11. Takimoto E, Kass DA. Role of oxidative stress in cardiac hypertrophy and remodeling. *Hypertension*. 2007;49:241–248.
12. Lassègue B, San Martín A, Griendling KK. Biochemistry, physiology, and pathophysiology of NADPH oxidases in the cardiovascular system. *Circ Res*. 2012;110:1364–1390.
13. Takano H, Zou Y, Hasegawa H, Akazawa H, Nagai T, Komuro I. Oxidative stress-induced signal transduction pathways in cardiac myocytes: involvement of ROS in heart diseases. *Antioxid Redox Signal*. 2003;5:789–794.
14. Higashi M, Shimokawa H, Hattori T, Hiroki J, Mukai Y, Morikawa K, Ichiki T, Takahashi S, Takeshita A. Long-term inhibition of Rho-kinase suppresses angiotensin II-induced cardiovascular hypertrophy in rats in vivo: effect on endothelial NAD(P)H oxidase system. *Circ Res*. 2003;93:767–775.
15. Zhou Q, Gensch C, Liao JK. Rho-associated coiled-coil-forming kinases (ROCKs): potential targets for the treatment of atherosclerosis and vascular disease. *Trends Pharmacol Sci*. 2011;32:167–173.
16. Brakebusch C, Fässler R. The integrin-actin connection, an eternal love affair. *EMBO J*. 2003;22:2324–2333.
17. Zhao XH, Laschinger C, Arora P, Szászi K, Kapus A, McCulloch CA. Force activates smooth muscle alpha-actin promoter activity through the Rho signaling pathway. *J Cell Sci*. 2007;120(Pt 10):1801–1809.
18. Nagai T, Anzai T, Kaneko H, Mano Y, Anzai A, Maekawa Y, Takahashi T, Meguro T, Yoshikawa T, Fukuda K. C-reactive protein overexpression exacerbates pressure overload-induced cardiac remodeling through enhanced inflammatory response. *Hypertension*. 2011;57:208–215.
19. Patel VB, Wang Z, Fan D, Zhabyeyev P, Basu R, Das SK, Wang W, Desaulniers J, Holland SM, Kassiri Z, Oudit GY. Loss of p47phox subunit enhances susceptibility to biomechanical stress and heart failure because of dysregulation of cortactin and actin filaments. *Circ Res*. 2013;112:1542–1556.
20. Qipshidze N, Tyagi N, Metreveli N, Lominadze D, Tyagi SC. Autophagy mechanism of right ventricular remodeling in murine model of pulmonary artery constriction. *Am J Physiol Heart Circ Physiol*. 2012;302:H688–H696.
21. Kehat I, Molkentin JD. Extracellular signal-regulated kinase 1/2 (ERK1/2) signaling in cardiac hypertrophy. *Ann N Y Acad Sci*. 2010;1188:96–102.
22. Nishida M, Maruyama Y, Tanaka R, Kontani K, Nagao T, Kurose H. Gα(i) and Gα(o) are target proteins of reactive oxygen species. *Nature*. 2000;408:492–495.
23. Scherz-Shouval R, Elazar Z. Regulation of autophagy by ROS: physiology and pathology. *Trends Biochem Sci*. 2011;36:30–38.
24. Okamoto R, Li Y, Noma K, Hiroi Y, Liu PY, Taniguchi M, Ito M, Liao JK. FHL2 prevents cardiac hypertrophy in mice with cardiac-specific deletion of ROCK2. *FASEB J*. 2013;27:1439–1449.
25. Zhang YM, Bo J, Taffet GE, Chang J, Shi J, Reddy AK, Michael LH, Schneider MD, Entman ML, Schwartz RJ, Wei L. Targeted deletion of ROCK1 protects the heart against pressure overload by inhibiting reactive fibrosis. *FASEB J*. 2006;20:916–925.
26. Brooks WW, Bing OH, Blaustein AS, Allen PD. Comparison of contractile state and myosin isozymes of rat right and left ventricular myocardium. *J Mol Cell Cardiol*. 1987;19:433–440.
27. Litten RZ, Martin BJ, Buchthal RH, Nagai R, Low RB, Alpert NR. Heterogeneity of myosin isozyme content of rabbit heart. *Circ Res*. 1985;57:406–414.
28. Takefuji M, Krüger M, Sivaraj KK, Kaibuchi K, Offermanns S, Wettschureck N. RhoGEF12 controls cardiac remodeling by integrating G protein- and integrin-dependent signaling cascades. *J Exp Med*. 2013;210:665–673.
29. Shi J, Wei L. Rho kinase in the regulation of cell death and survival. *Arch Immunol Ther Exp (Warsz)*. 2007;55:61–75.
30. Thumkeo D, Keel J, Ishizaki T, Hirose M, Nonomura K, Oshima H, Oshima M, Taketo MM, Narumiya S. Targeted disruption of the mouse rho-associated kinase 2 gene results in intrauterine growth retardation and fetal death. *Mol Cell Biol*. 2003;23:5043–5055.
31. Liang Q, Wiese RJ, Bueno OF, Dai YS, Markham BE, Molkentin JD. The transcription factor GATA4 is activated by extracellular signal-regulated kinase 1- and 2-mediated phosphorylation of serine 105 in cardiomyocytes. *Mol Cell Biol*. 2001;21:7460–7469.
32. Akazawa H, Komuro I. Roles of cardiac transcription factors in cardiac hypertrophy. *Circ Res*. 2003;92:1079–1088.
33. Perrino C, Rockman HA. GATA4 and the two sides of gene expression reprogramming. *Circ Res*. 2006;98:715–716.
34. Suzuki YJ. Cell signaling pathways for the regulation of GATA4 transcription factor: Implications for cell growth and apoptosis. *Cell Signal*. 2011;23:1094–1099.
35. Yanazume T, Hasegawa K, Wada H, Morimoto T, Abe M, Kawamura T, Sasayama S. Rho/ROCK pathway contributes to the activation of extracellular signal-regulated kinase/GATA-4 during myocardial cell hypertrophy. *J Biol Chem*. 2002;277:8618–8625.
36. Lawrie A, Spiekerkoetter E, Martinez EC, Ambartsumian N, Sheward WJ, MacLean MR, Harmar AJ, Schmidt AM, Lukanidin E, Rabinovitch M. Interdependent serotonin transporter and receptor pathways regulate S100A4/Mts1, a gene associated with pulmonary vascular disease. *Circ Res*. 2005;97:227–235.
37. Liu Y, Suzuki YJ, Day RM, Fanburg BL. Rho kinase-induced nuclear translocation of ERK1/ERK2 in smooth muscle cell mitogenesis caused by serotonin. *Circ Res*. 2004;95:579–586.
38. Nakai A, Yamaguchi O, Takeda T, Higuchi Y, Hikoso S, Taniike M, Omiya S, Mizote I, Matsumura Y, Asahi M, Nishida K, Hori M, Mizushima N, Otsu K. The role of autophagy in cardiomyocytes in the basal state and in response to hemodynamic stress. *Nat Med.* 2007;13:619–624.
39. Nishida K, Kyoi S, Yamaguchi O, Sadoshima J, Otsu K. The role of autophagy in the heart. *Cell Death Differ*. 2009;16:31–38.
40. Satoh K, Fukumoto Y, Shimokawa H. Rho-kinase: important new therapeutic target in cardiovascular diseases. *Am J Physiol Heart Circ Physiol*. 2011;301:H287–H296.
41. Fukumoto Y, Yamada N, Matsubara H, et al. Double-blind, placebo-controlled clinical trial with a rho-kinase inhibitor in pulmonary arterial hypertension. *Circ J*. 2013;77:2619–2625.
42. Simon MA. Assessment and treatment of right ventricular failure. *Nat Rev Cardiol*. 2013;10:204–218.
43. Hardziyenka M, Campian ME, Reesink HJ, Surie S, Bouma BJ, Groenink M, Klemens CA, Beekman L, Remme CA, Bresser P, Tan HL. Right ventricular failure following chronic pressure overload is associated with reduction in left ventricular mass: evidence for atrophic remodeling. *J Am Coll Cardiol*. 2011;57:921–928.
44. Ross J Jr. Acute displacement of the diastolic pressure-volume curve of the left ventricle: role of the pericardium and the right ventricle. *Circulation*. 1979;59:32–37.

Significance

Right ventricular (RV) failure is the leading cause of death in various cardiopulmonary diseases, including pulmonary hypertension. However, as compared with left ventricular (LV) failure, the molecular mechanisms of RV failure are poorly understood, and hence therapeutic targets of the disorder remain to be elucidated. Because RV failure actually does not accord with LV failure, the development of the specialized therapy of RV failure may improve the prognosis of the patients. Therefore, we aimed to identify specialized molecular therapeutic targets for pressure overload–induced RV failure by comparing the responses of both ventricles in mice. In this study, by microarray analysis, we identified the significant upregulations of the molecules related to the Rho-kinase and integrin pathways in the pressure-loaded RV. Additionally, we show that the Rho-kinase pathway (especially ROCK2-mediated one) plays a crucial role in RV hypertrophy and dysfunction, suggesting that the pathway is a novel therapeutic target of RV failure in humans.

Arteriosclerosis, Thrombosis, and Vascular Biology

JOURNAL OF THE AMERICAN HEART ASSOCIATION

Crucial Role of Rho-Kinase in Pressure Overload–Induced Right Ventricular Hypertrophy and Dysfunction in Mice

Shohei Ikeda, Kimio Satoh, Nobuhiro Kikuchi, Satoshi Miyata, Kota Suzuki, Junichi Omura, Toru Shimizu, Kenta Kobayashi, Kazuto Kobayashi, Yoshihiro Fukumoto, Yasuhiko Sakata and Hiroaki Shimokawa

Arterioscler Thromb Vasc Biol. 2014;34:1260-1271; originally published online March 27, 2014;
doi: 10.1161/ATVBAHA.114.303320
Arteriosclerosis, Thrombosis, and Vascular Biology is published by the American Heart Association, 7272 Greenville Avenue, Dallas, TX 75231

Print ISSN: 1079-5642. Online ISSN: 1524-4636

Supplementary Figure I

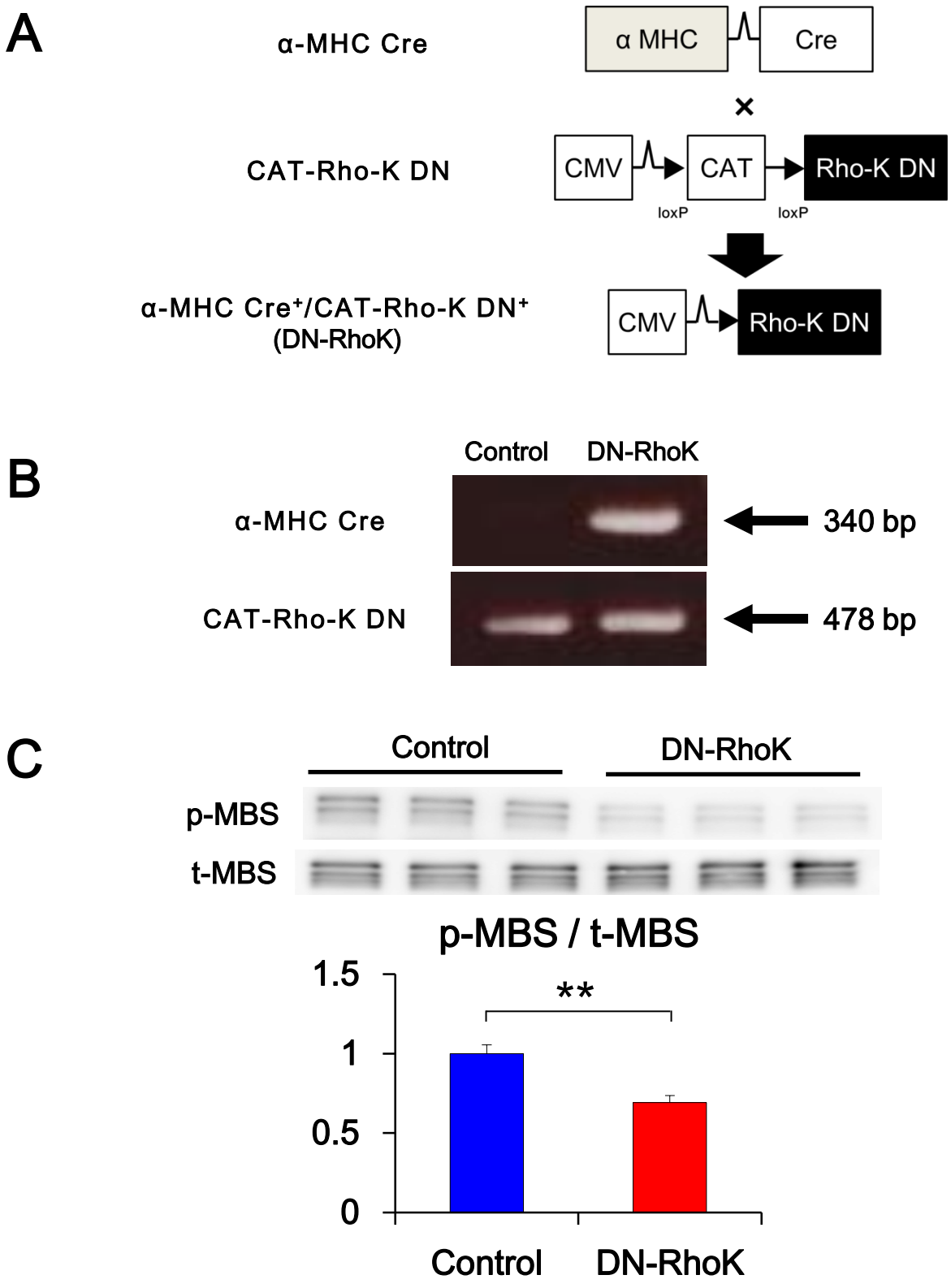

Supplementary Figure I. Generation of DN-RhoK Mice

(A) Male mice containing the Rho-kinase dominant-negative mutant were crossed with female heterozygous α-MHC promoter-driven Cre recombinase transgenic mice. **(B)** PCR amplification products of genomic DNA from mouse heart, confirming the presence of the DN-RhoK mutant and α-MHC Cre recombinase in DN-RhoK mice. **(C)** Representative Western blotting and quantitative analysis of phospho-MBS (p-MBS) and total MBS (t-MBS) in the RV tissues (n=6 each). Results are expressed as mean ± SEM. **P<0.01.

Supplementary Figure II

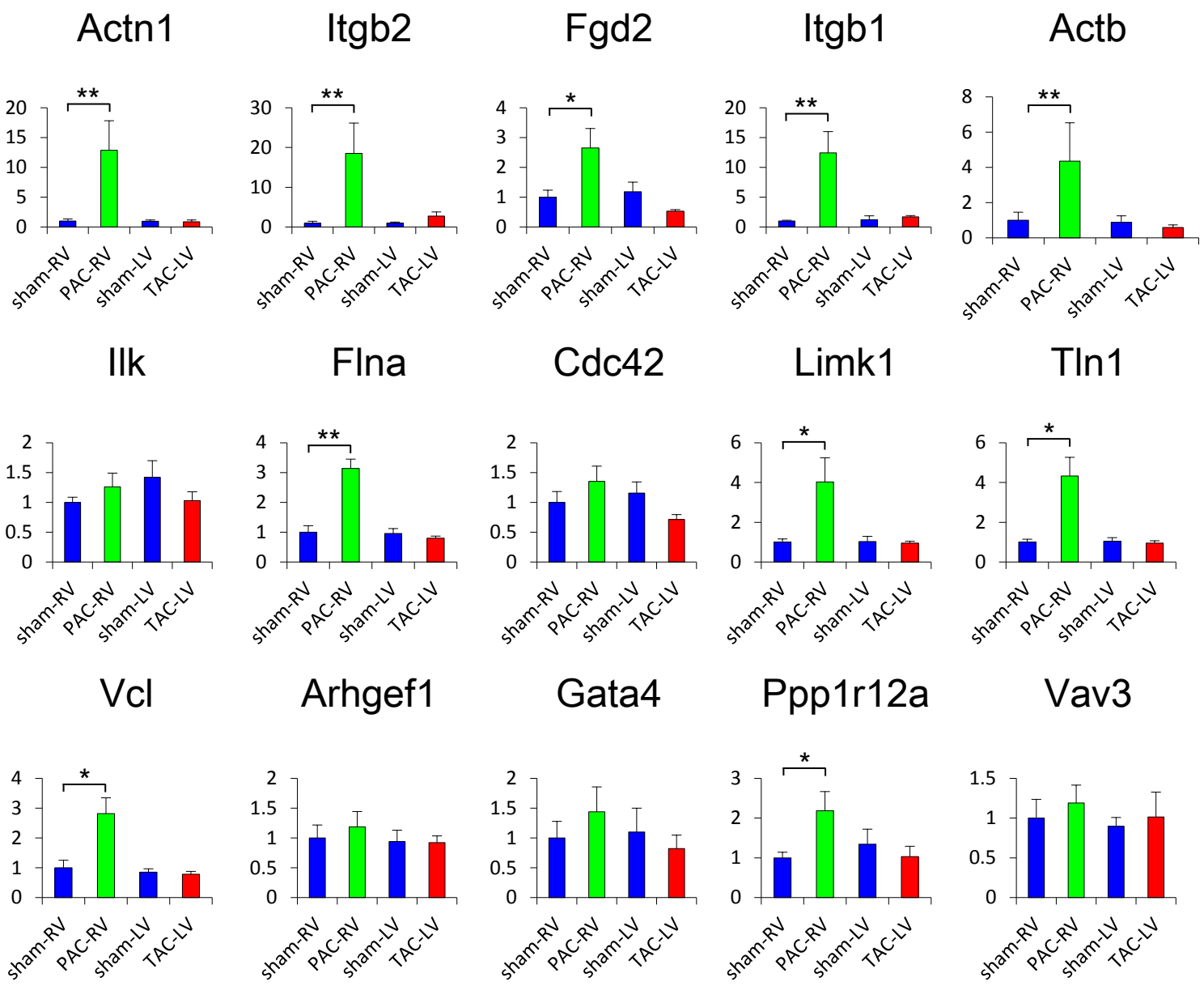

Supplementary Figure II. mRNA expressions of top 15 genes by the microarray analysis

The gene expressions in the RV after PAC and those in the LV after TAC as well as the respective controls (sham). Results are adjusted by GAPDH. Results are expressed as mean ± SEM. *P<0.05, **P<0.01 (*n*=6 each).

Supplementary Figure III

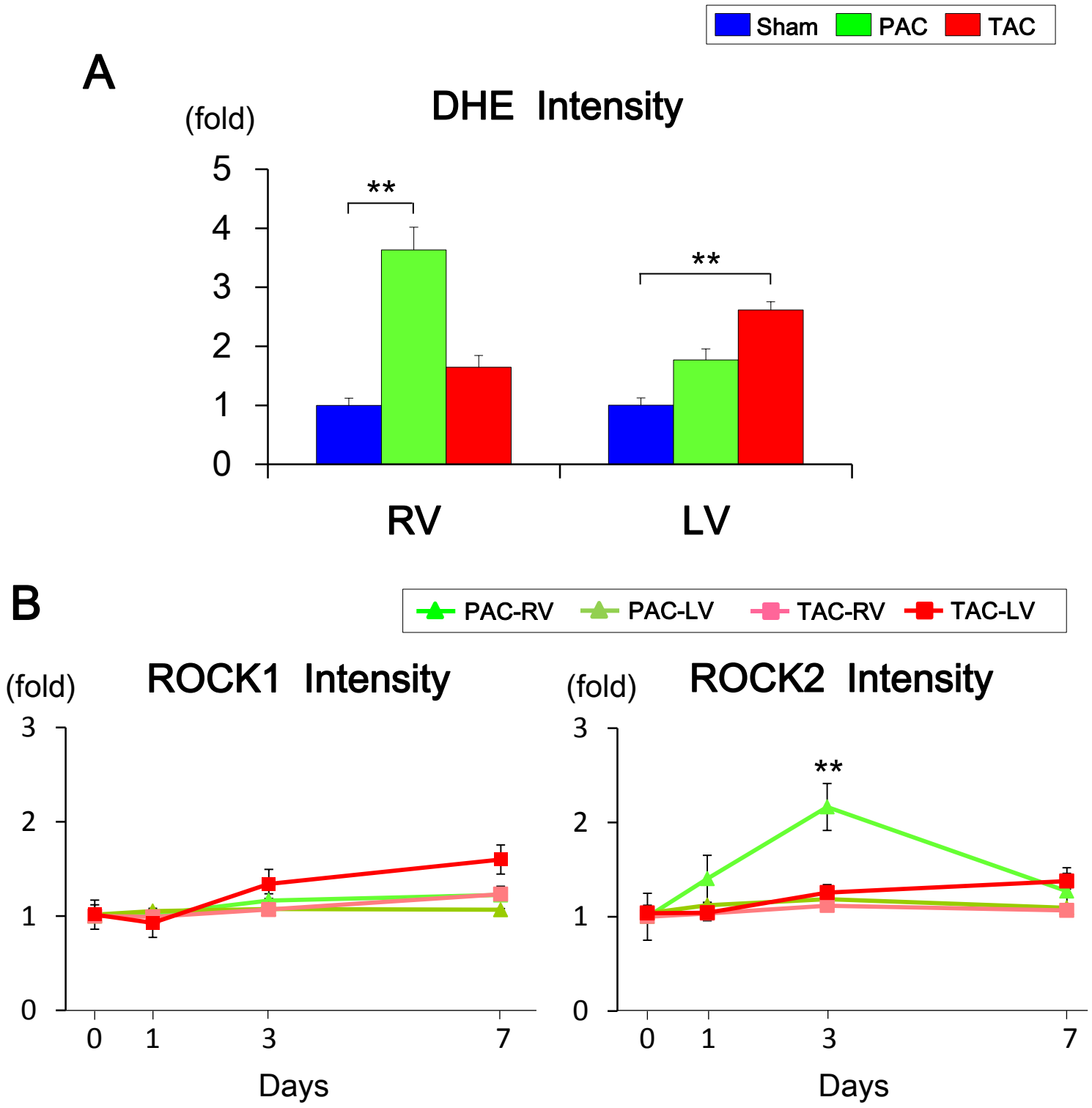

Supplementary Figure III. Pressure-Overload-Induced Oxidative Stress and Rho-kinase in the Ventricles

(**A**) Quantification of DHE staining intensity (*n*=5 each). The intensity was significantly up-regulated in the pressure-loaded ventricles, especially RV after PAC. (**B**) Quantification of ROCK1 and 2 immunostaining intensity (*n*=5 each). The intensity of ROCK2 significantly increased at the day3 after PAC. Results are expressed as mean ± SEM. *P<0.05, **P<0.01 vs. day 0.

Supplementary Figure IV

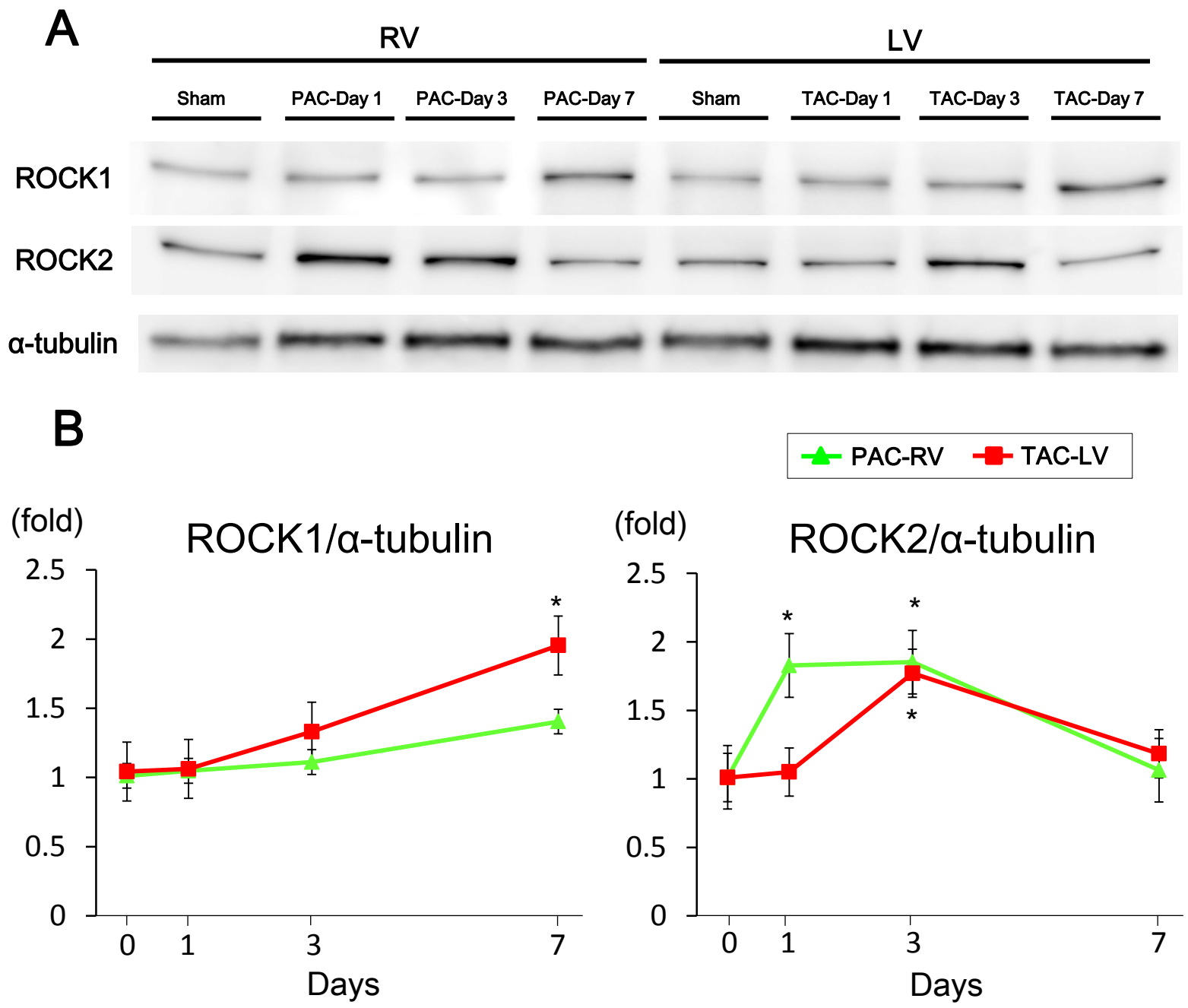

Supplementary Figure IV. Pressure-Overload-regulated Rho-kinase protein levels in the Ventricles

(A, B) Representative western blotting photographs of ROCK1 and 2 and quantitative analysis of the protein levels of ROCK1 and 2 in the time-course after operation (*n*=5 each). The protein levels of ROCK2 were significantly up-regulated in the day1 and day3 after PAC and in the day3 after TAC. On the other hand, the protein levels of ROCK1 increased gradually after PAC and TAC. Especially, the ROCK1 level at the day7 after TAC was significantly up-regulated. Results are expressed as mean ± SEM. *P<0.05, **P<0.01 vs. day 0.

Supplementary Figure V

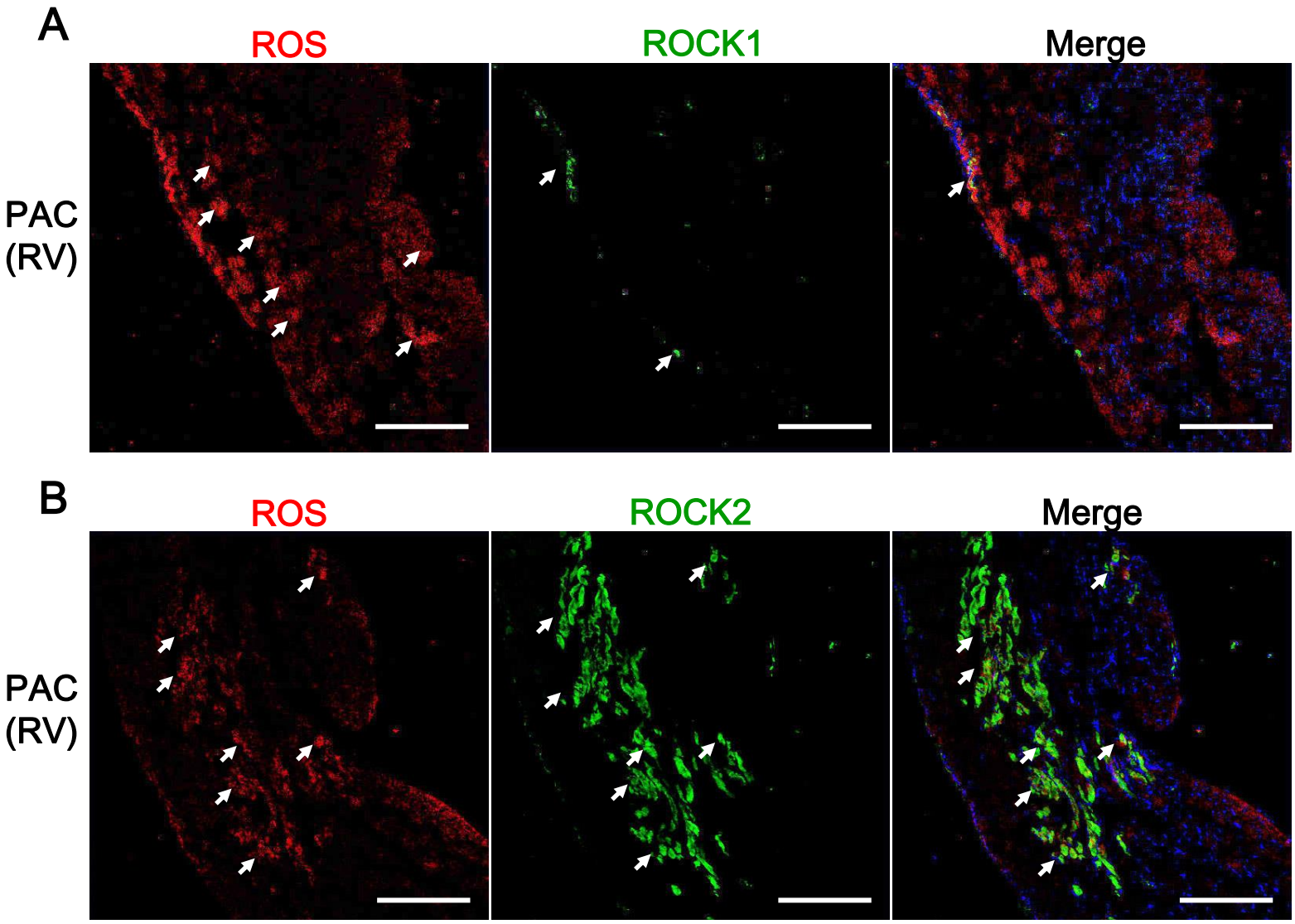

Supplementary Figure V. Relationship between Pressure-Overload-Induced Oxidative Stress and Rho-kinases Expression

Representative photomicrographs of double-staining showing relationships between oxidative stress and Rho-kinases expression in the RV free wall at day 1 after PAC. There was a co-localization of reactive oxygen species (ROS) and ROCK2 (but not ROCK1) in the RV after PAC. (**A**) Double-staining for ROS and ROCK1 (ROS, CellROX deep red; ROCK1, Alexa Fluor 488-green; DAPI, blue). (**B**) Double-staining for ROS and ROCK2 (ROS, CellROX deep red; ROCK2, Alexa Fluor 488-green; DAPI, blue). Scale bars, 200 μm.

Supplementary Figure VI

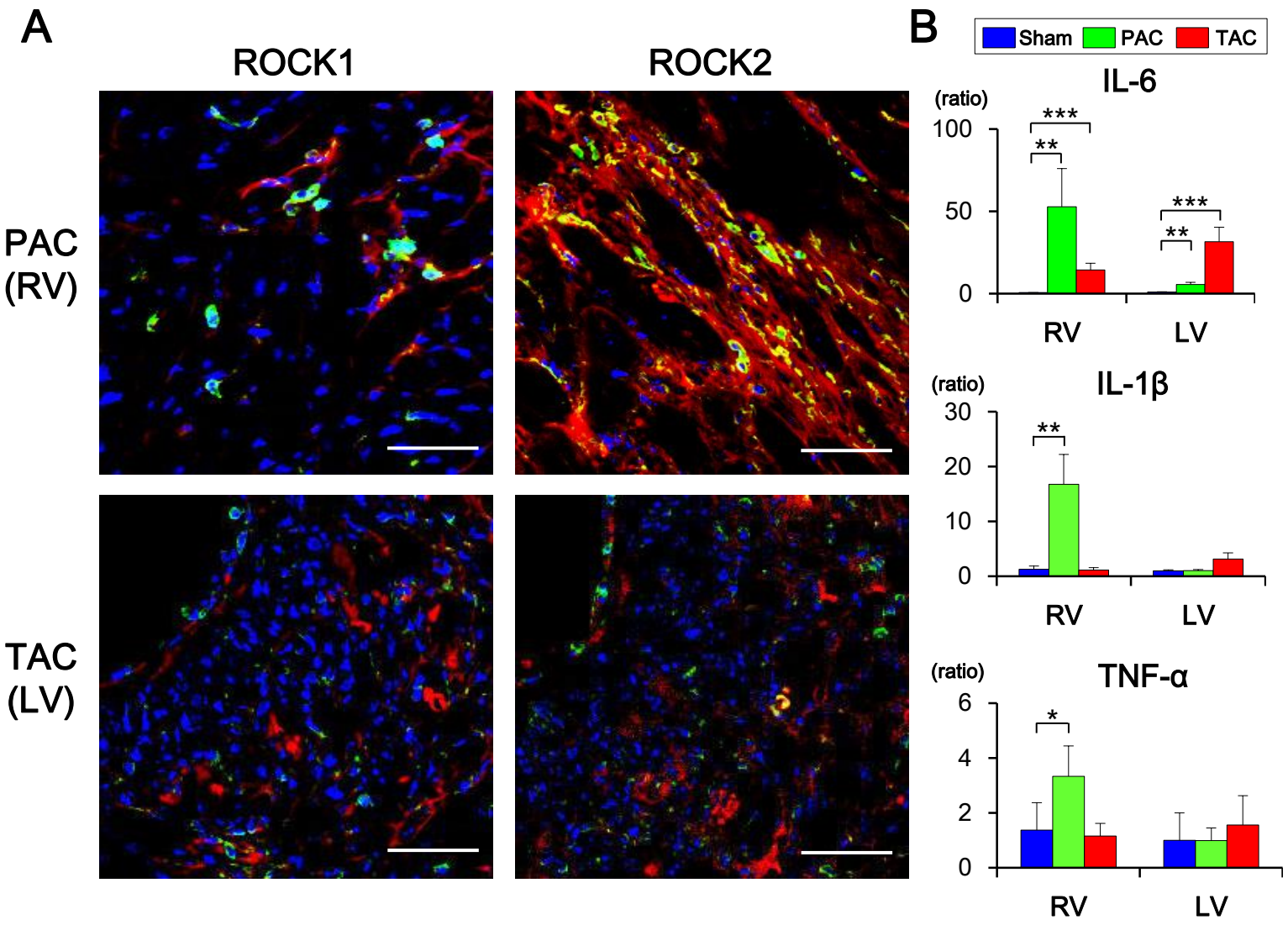

Supplementary Figure VI. Pressure-Overload-Induced Rho-kinase Up-regulation and Inflammatory Cell Migration

(**A**) Representative photomicrographs of double-immunostaining of Rho-kinases and CD45 expression at day 7 in the RV after PAC and the LV after TAC (ROCK1/ROCK2, Alexa Fluor 633-red; CD45, Alexa Fluor 488-green; DAPI, blue). PAC induced strong ROCK2 (but not ROCK1) expression exclusively in the RV, accompanied with CD45-positive inflammatory cell migration. Scale bars, 100 μm. (**B**) Relative mRNA expressions of inflammatory gene (e.g. IL-6, IL-1β, TNF-α) in both ventricles 24hours after PAC or TAC compared with control (n=10~12 each). There were significant increases in inflammatory gene expressions in the loaded ventricles, especially higher in the RV after PAC. Results are adjusted by GAPDH. Results are expressed as mean ± SEM. *P<0.05, **P<0.01, ***P<0.001. IL-6, interleukin-6; IL-1β, interleukin-1b; TNF-α, tumor necrosis factor-a.

Supplementary Figure VII

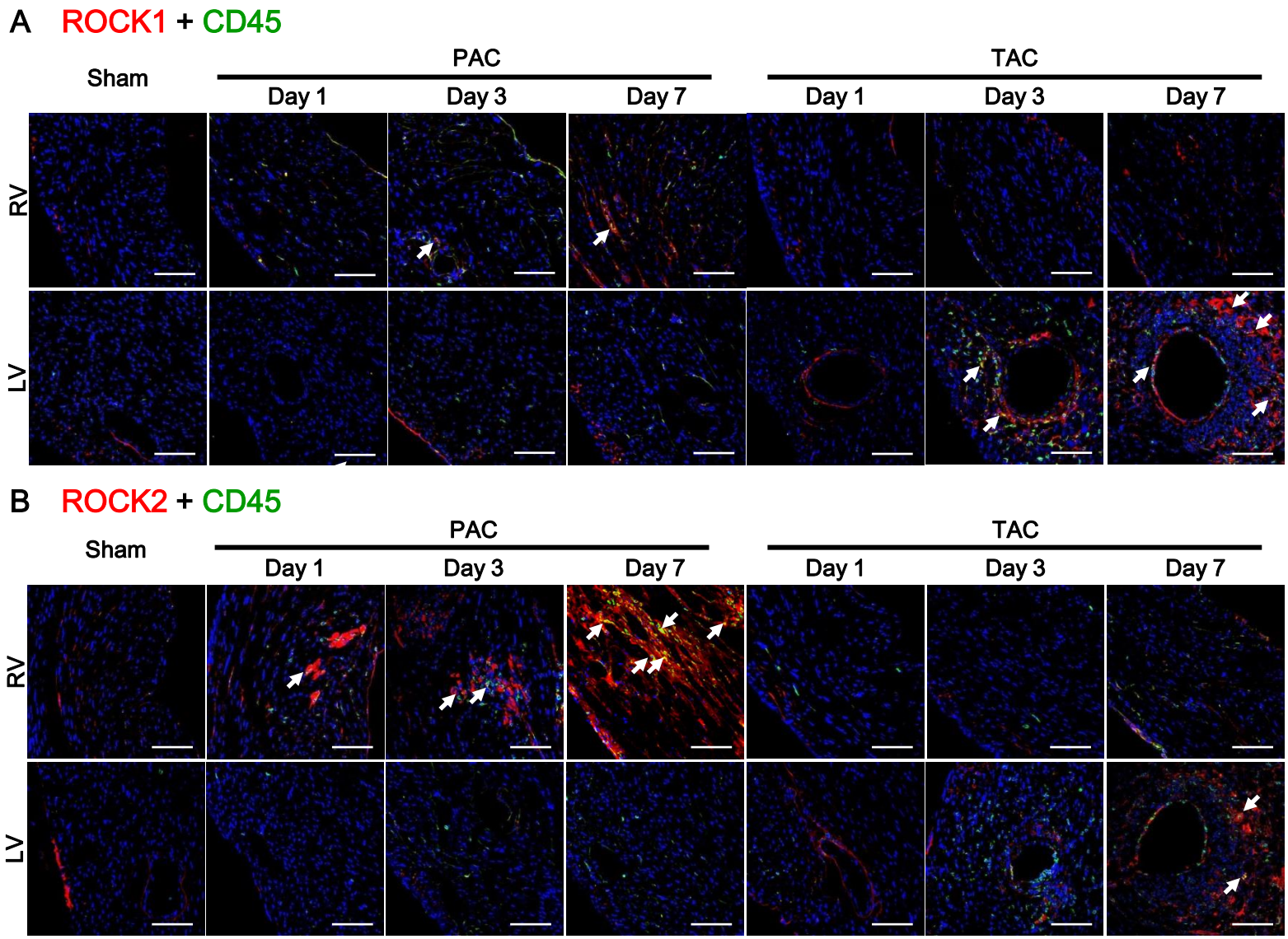

Supplementary Figure VII. Relationship between Pressure-Overload-Induced Rho-kinase Up-regulation and Inflammation

Representative photomicrographs of double-immunostaining showing time-course and localization of Rho-kinases and CD45 expression after PAC or TAC. PAC progressively induced strong ROCK2 expression in the RV from day 1, accompanied with CD45-positive cells. In contrast, TAC induced ROCK1 and ROCK2 expressions in the perivascular wall at day 7, accompanied with CD45-positive cells gently. (**A**) Double-immunostaining for ROCK1 and CD45 (ROCK1, Alexa Fluor 633-red; CD45, Alexa Fluor 488-green; DAPI, blue). (**B**) Double-immunostaining for ROCK2 and CD45 (ROCK2, Alexa Fluor 633-red; CD45, Alexa Fluor 488-green; DAPI, blue). Scale bars, 100 μm.

Supplementary Figure VIII

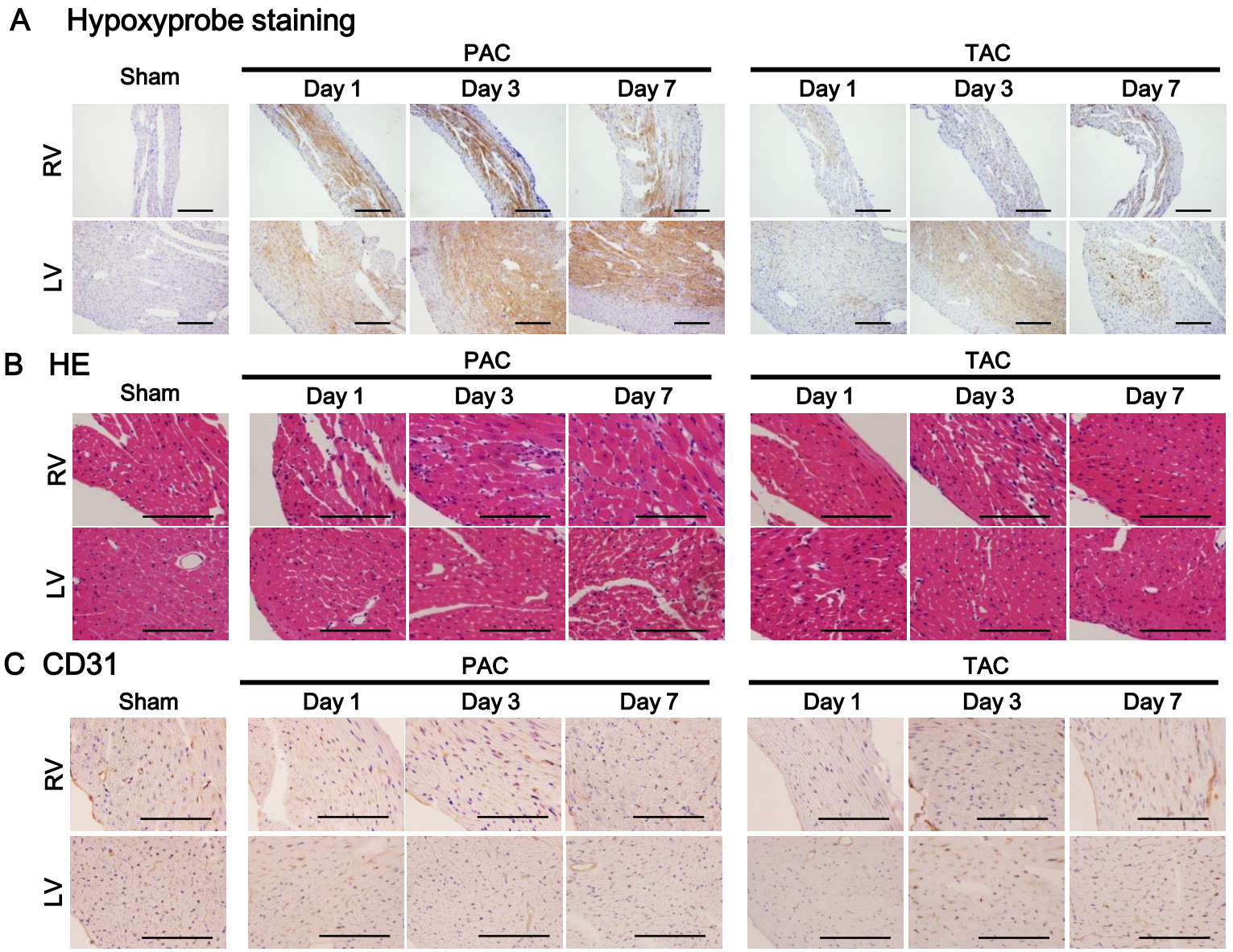

Supplementary Figure VIII. Pressure-Overload-Induced Ischemic Change and Cardiac Hypertrophy

(**A**) Representative photomicrographs of a hypoxyprobe staining in the RV and the LV show the time-course ischemic change after PAC or TAC. Scale bars, 200 μm. PAC and TAC induced myocardial ischemic change, especially apparent from day 1 after PAC. (**B**) Representative photomicrographs of hematoxylin-eosin staining of the RV and the LV after PAC or TAC. PAC and TAC significantly induced progressive cardiac hypertrophy in the loaded ventricles. Scale bars, 100 μm. (**C**) Representative photomicrographs of immunostaining for CD31 of the RV and the LV after PAC or TAC. PAC reduced the capillaries in the RV in the time-course, in contrast TAC increased capillaries in the LV. Scale bars, 100 μm.

Supplementary Figure IX

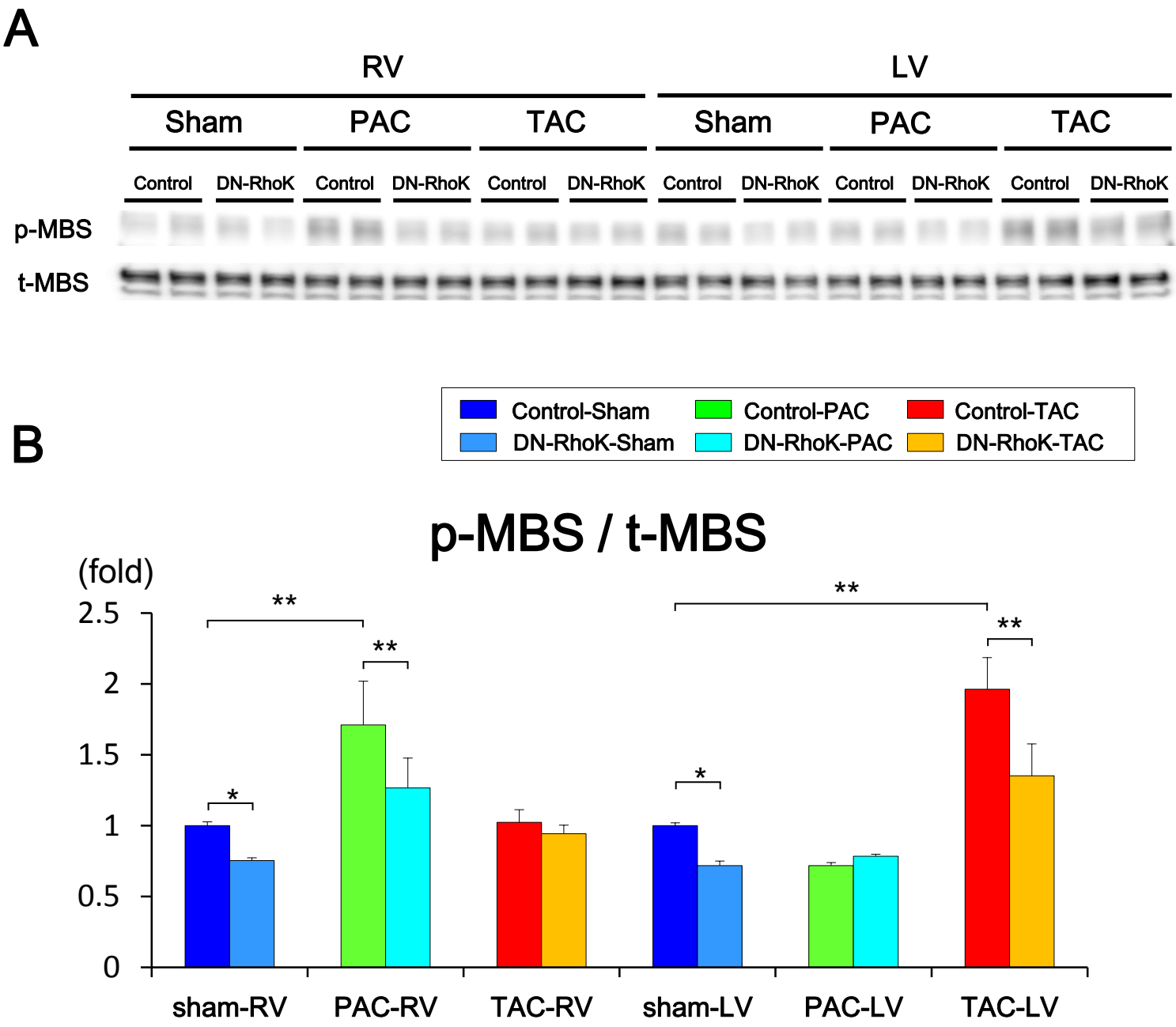

Supplementary Figure IX. Pressure-Overload Activates myocardial Rho-kinase

(A, B) Representative western blotting photographs of phospho-MBS (p-MBS) and total MBS (t-MBS) and quantitative analysis of Rho-kinase activity in both ventricles 4 weeks after operation (*n*=5 each). PAC and TAC significantly activated Rho-kinase in pressure-loaded ventricles, and the respective activations were significantly less in DN-RhoK mice compared with controls. In contrast, the contralateral ventricles to pressure-overload (LV after PAC and RV after TAC) had no Rho-kinase activation. Results are expressed as mean ± SEM. *P<0.05, **P<0.01.

Supplementary Figure X

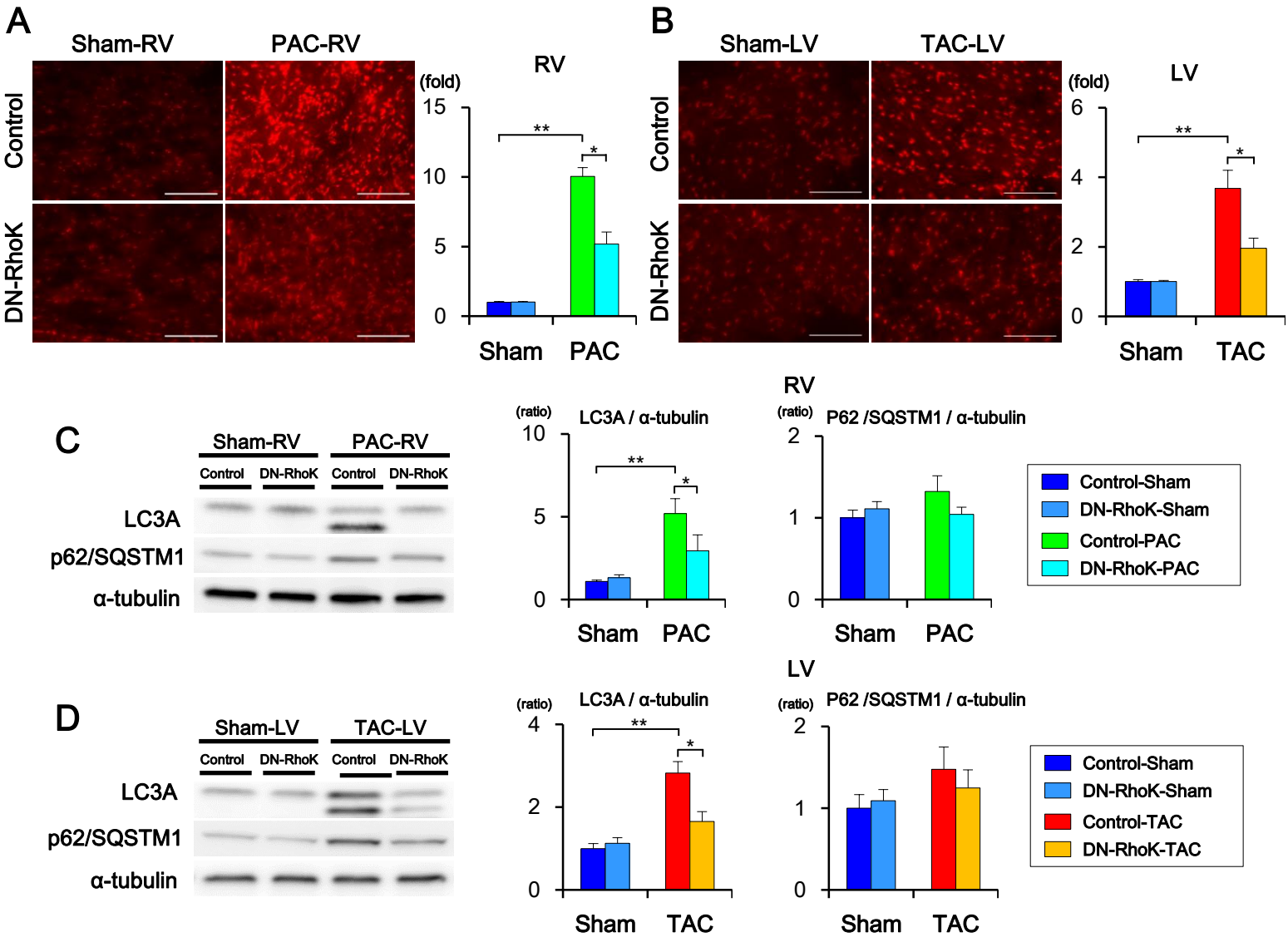

Supplementary Figure X. Rho-kinase Enhances Myocardial Oxidative Stress in Response to Pressure-Overload

(A, B) Representative photomicrographs and quantification of DHE staining of loaded ventricles 4 weeks after operation (*n*=6 each). PAC and TAC significantly induced oxidative stress in the pressure-loaded ventricles, especially in the RV after PAC. However, the respective fluorescence intensities were significantly less in DN-RhoK compared with controls. Scale bars, 100 μm.

(C, D) Representative Western blotting of LC3A and p62/SQSTM1 in loaded ventricles 4 weeks after operation (*n*=6 each). PAC and TAC significantly increased the levels of LC3A in pressure-loaded ventricles, and the increase was significantly less in DN-RhoK mice compared with controls. The level of p62/SQSTM1 was not significantly altered. Results are expressed as mean ± SEM. *P<0.05, **P<0.01.

Supplementary Figure XI

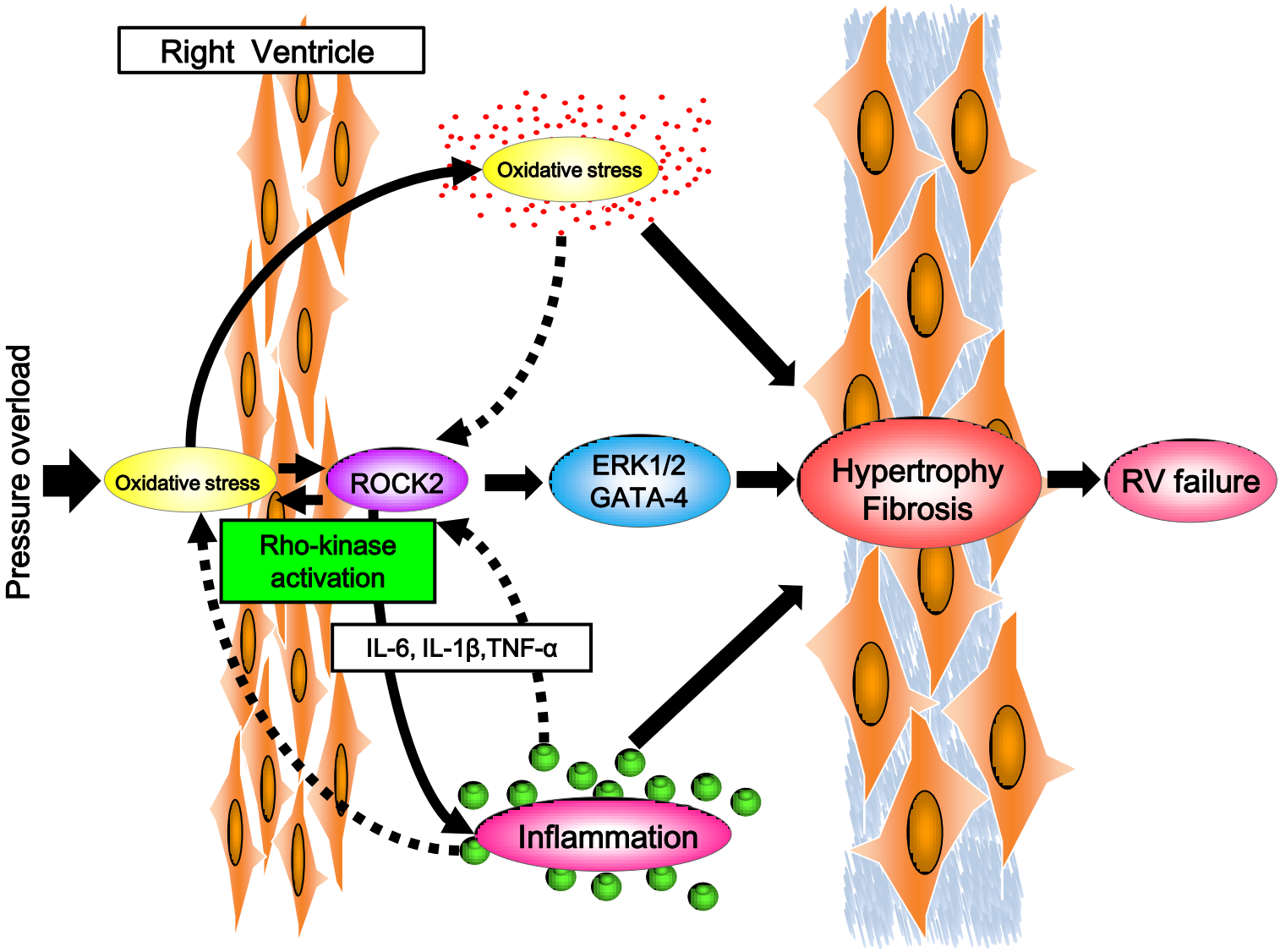

Supplementary Figure XI. Crucial Role of Rho-kinase in Pressure-Overload-Induced Right Ventricular Hypertrophy and Dysfunction

RV Pressure-overload activates Rho-kinases and induces oxidative stress, which then immediately affects Rho-kinases expression, especially ROCK2. Accompanying inflammatory responses, myocardial Rho-kinase plays a crucial role for activation of ERK1/2-GATA4 signaling in response to pressure-overload. As a result, Rho-kinase deteriorates cardiac function and survival after PAC.

Supplementary Figure XII

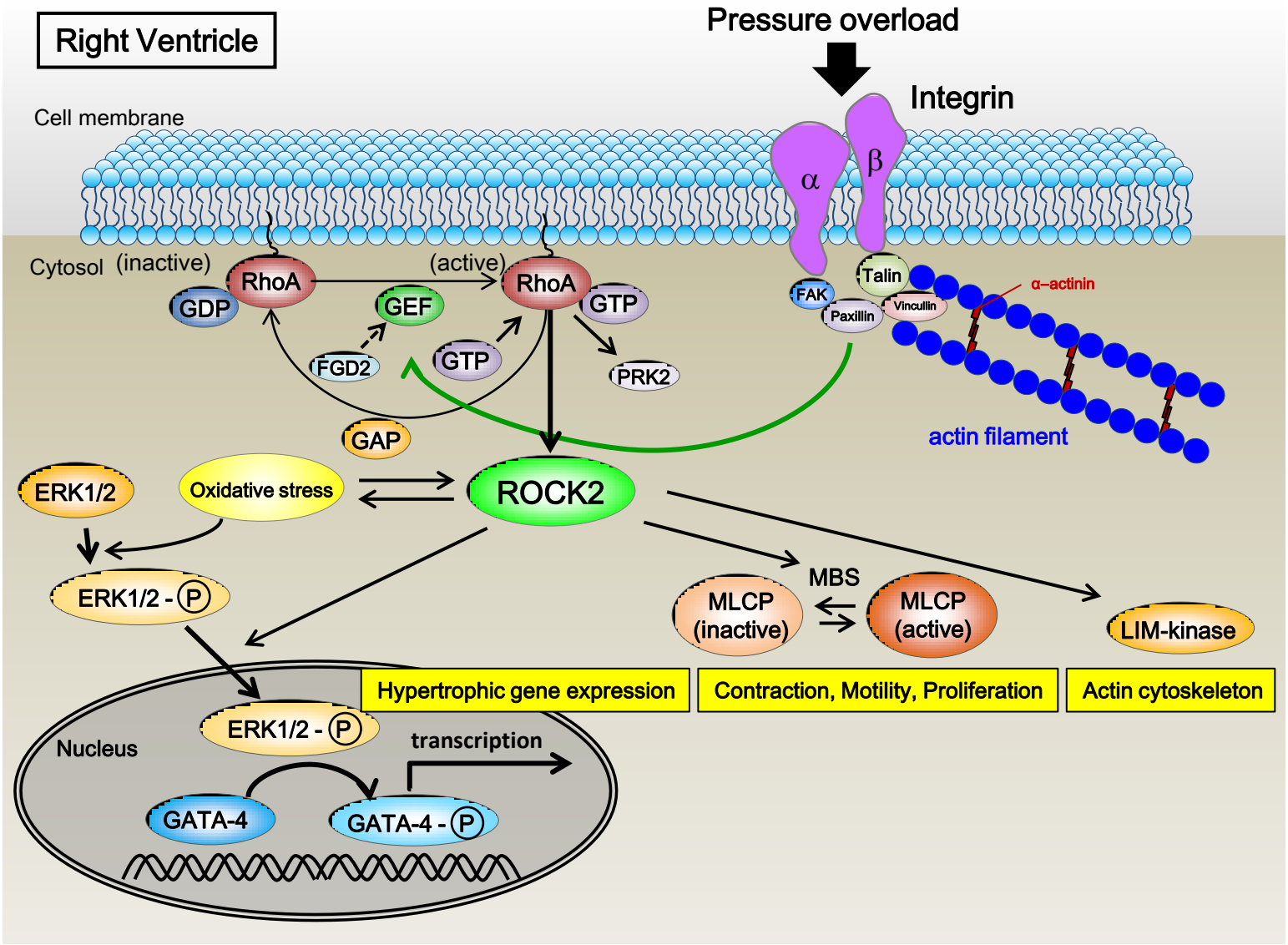

Supplementary Figure XII. The RhoA/ROCK2 Signaling Pathway Activated by RV Pressure-Overload RV Pressure-overload stimulates integrin and integrin-related adhesion components through mechanical stretch. RV Pressure-overload then activates the guanine nucleotide exchange factors (GEFs) that catalyze exchange of GDP for GTP, and then activates RhoA. The active RhoA interacts with several downstream targets, including ROCK2 and PRK2. Through the induction of oxidative stress, RV pressure-overload activated several substrates of Rho-kinase, such as myosin binding subunit (MBS) and LIM-kinase. Additionally, Rho-kinase translocates phospho-ERK into the nucleus, where ERK then phosphorylates GATA4. Finally, Rho-kinase activation is involved in the regulation of the various fundamental cellular functions including contraction, motility, proliferation, actin cytoskeleton, and hypertrophic gene expression. FAK, Focal adhesion kinase, (gene symbol: Ptk2); FGD2, FYVE, RhoGEF and PH domain-containing protein 2, (gene symbol: Fgd2); PRK2, protein kinase C-related kinases, (gene symbol: Pkn2); MBS, myosin binding subunit, (gene symbol: Ppp1r12a); ERK, Extracellular signal-regulated kinase, (gene symbol: Mapk1)

Supplementary Tables

Supplementary Table I. Baseline Characteristics of Mice

Parameters	Control (n = 6)	DN-RhoK (n = 6)	P-value
Body Weight (g)	24.6 ± 0.20	24.5 ± 0.20	N.S.
Tibial Length (mm)	17.1 ± 0.07	17.0 ± 0.11	N.S.
HW/BW (mg/g)	5.06 ± 0.07	5.10 ± 0.08	N.S.
RV W/BW (mg/g)	1.05 ± 0.03	1.06 ± 0.03	N.S.
LV+S W/BW (mg/g)	3.59 ± 0.10	3.52 ± 0.05	N.S.
RV/LV+S (fold)	0.29 ± 0.01	0.30 ± 0.01	N.S.
Systolic BP (mmHg)	104.4 ± 3.4	104.2 ± 3.3	N.S.

Results are expressed as mean ± SEM. Comparisons were made using one-way ANOVA.

Supplementary Table II. Characteristics of Mice at 4 weeks after Operation

Parameters	Sham		PAC		TAC	
	Control (n = 8)	DN-RhoK (n = 8)	Control (n = 8)	DN-RhoK (n = 8)	Control (n = 8)	DN-RhoK (n = 8)
Body Weight (g)	26.0 ± 0.30	25.7 ± 0.24	24.7 ± 0.30	24.9 ± 0.40	25.5 ± 0.30	25.4 ± 0.20
HW/BW (mg/g)	4.89 ± 0.05	4.90 ± 0.05	5.73 ± 0.09 *	5.69 ± 0.09 †	7.37 ± 0.06 *	7.10 ± 0.09 † §
RV W/BW (mg/g)	1.04 ± 0.02	1.07 ± 0.02	1.75 ± 0.03 *	1.56 ± 0.02 † ‡‡	1.18 ± 0.03 *	1.10 ± 0.04 §
RV/LV + S (mg/mg)	0.30 ± 0.01	0.31 ± 0.01	0.55 ± 0.01 *	0.47 ± 0.01 † ‡‡	0.21 ± 0.02 *	0.21 ± 0.02 †
LV + S W/BW (mg/g)	3.49 ± 0.03	3.53 ± 0.05	3.18 ± 0.04 *	3.34 ± 0.06 ‡	5.67 ± 0.06 *	5.27 ± 0.07 † §§
Liver W/BW (mg/g)	40.0 ± 1.34	39.6 ± 1.08	48.8 ± 1.85 *	44.2 ± 1.66 † ‡	41.4 ± 1.24	40.9 ± 1.13
Lung W/BW (mg/g)	7.13 ± 0.26	7.08 ± 0.27	7.30 ± 0.22	7.33 ± 0.19	10.2 ± 0.27 *	8.23 ± 0.40 † §

Results are expressed as mean ± SEM. HW, heart weight; BW, body weight; LV W, left ventricle weight; S W, Septum weight; RV W, right ventricle weight. Comparisons were made using one-way ANOVA. *P<0.01 vs. sham-operated controls; †P<0.01 vs. sham-operated DN-RhoK mice; ‡P<0.05, ‡‡P<0.01 vs. controls with PAC; §P<0.05, §§P<0.01 vs. controls with TAC

Supplementary Table III. Plasma Levels of Liver Enzymes at 4 weeks after Operation

Parameters	Sham		PAC		TAC	
	Control (n = 8)	DN-RhoK (n = 8)	Control (n = 8)	DN-RhoK (n = 8)	Control (n = 8)	DN-RhoK (n = 8)
T-bil (mg/dl)	0.51 ± 0.03	0.50 ± 0.03	0.91 ± 0.12 *	0.64 ± 0.03 ‡	0.55 ± 0.04	0.57 ± 0.07
AST (U/ml)	43.4 ± 1.29	45.3 ± 2.05	90.1 ± 12.9 *	46.9 ± 4.15 † ‡‡	40.0 ± 2.42	45.5 ± 1.86
ALT (U/ml)	26.3 ± 1.24	26.1 ± 1.24	55.3 ± 2.89 *	48.9 ± 2.92 †	25.3 ± 0.62	26.9 ± 0.81
ALB (g/dl)	2.26 ± 0.06	2.31 ± 0.04	2.69 ± 0.07 *	2.58 ± 0.07	2.44 ± 0.03	2.45 ± 0.09

Results are expressed as mean ± SEM. T-bil: Total bilirubin, AST: aspartate aminotransferase, ALT: alanine aminotransferase, ALB: albumin. Comparisons were performed using one-way ANOVA.

*$P < 0.01$ vs. sham-operated controls; †$P < 0.01$ vs. sham-operated DN-RhoK mice; ‡$P < 0.05$, ‡‡$P < 0.01$ vs. controls with PAC